

THE FLORIDA STATE UNIVERSITY  
COLLEGE OF ARTS AND SCIENCES

EVALUATION OF WIND PRODUCTS  
FOR FORCING COASTAL OCEAN MODELS

By

XUJING JIA

A Thesis submitted to the  
Department of Oceanography  
in partial fulfillment of the  
requirements for the degree of  
Master of Science

Degree Awarded:  
Fall Semester, 2002

Fall Semester, 2002

This thesis is dedicated to my family, my friends, all the people I love and all those who always care about me.

## ACKNOWLEDGEMENTS

I would like to thank my advisor Dr. James. J. O'Brien for all the guidance and support he has offered as well as the chance he presented me to study in the Center For Ocean-Atmospheric Studies. It has been a unique experience and I have truly learned a lot over the past two years.

I am indebted to Dr. Georges Weatherly and Dr. Richard Iverson for giving me their precious time and helping me improve my work during this busy summer semester. Their insight is valuable to both me and my work and has guided me well in my future career.

My deepest thanks go to Jorge Zavala. Throughout the course of my research, he has been an incredible coach, a mentor and a dedicated friend. Thanks also to Steve Morey, for his help, and presenting challenging issues for me to consider in the research process. Thanks should also be directed to Mark Bourassa, the creator of the QSCAT and HYBRID wind fields involved in my thesis, and his considerate help in developing an understanding in each of their nuances.

In addition to the people who have worked together with me on my thesis, I want to thank Dr. William Dewar for all the support and encouragement he has offered. Through the entire time I have spent at FSU, his belief in me has meant so much.

THANK DR. WILLIAM DEWAR FOR ALL THE SUPPORT AND ENCOURAGEMENT HE HAS OFFERED. THROUGH THE ENTIRE TIME I HAVE SPENT AT FSU, HIS BELIEF IN ME HAS MEANT SO MUCH.

Of course, I want to say a huge "thank you!" to the academic coordinator of oceanography department, Ms. Michaela Lupiani. She has helped me from the day I

applied FSU and even now, she has taken care of me and all of the needs I could possibly have. She will always be one of my truest friends. From her warm care and thoughtfulness, I have always felt at home although I am so far away from my family.

Indeed, it has been very hard to be away from my home and family during my stay here. No matter the distance though, it is my family who has given me the greatest gifts in life, their love, their belief in me, and the pride in watching their dreams and mine come true. My heart belongs to them, and especially Shannon, my husband, who has tirelessly worked with me, inspired me, and loved me more than I ever dreamed possible.

## TABLE OF CONTENTS

List of Tables .....	vii
List of Figures .....	viii
Abstract .....	ix
1. INTRODUCTION .....	1
2. DATA SETS .....	4
3. MODEL DESCRIPTION AND WIND FORCING EXPERIMENTS .....	10
4. RESULTS .....	14
5. CONCLUSION .....	23
REFERENCES .....	48
BIOGRAPHICAL SKETCH .....	51

LIST OF TABLES

1 a. Increase Rate of Correlation Coefficient of SSH after  
Inverse Barometer Correction Being Added .....47

1 b. Decrease Rate of RMSE of SSH after  
Inverse Barometer Correction Being Added ..... 47

## LIST OF FIGURES

1. Buoy Station Map .....	27
2. NCOM Vertical Coordinate System .....	28
3. Wind Stress Time Series (2 month examples) .....	29
4. Wind Stress Comparison between Observation and ETA, QSCAT and HYBRID .....	34
5. Wind Fields Snapshots from ETA, QSCAT and HYBRID .....	35
6. Wind Stress Time Series (for the whole study time period) .....	36
7. Wind Stress Comparison between Different Wind fields During Different Time Periods .....	37
8. The Map Where the Four Stations and NDBC Buoy are Located .....	38
9. SSH Time Series .....	39
10. Snapshots of The SSH fields .....	40
11. SSH Comparison for The Whole Study Time Period .....	41
12. SSH Time Series after Inverse Barometer Correction Being Added to Model Simulations.....	42
13. SSH Comparison for The Whole Study Time Period after Inverse Barometer Correction Being Added .....	43
14. SSH Comparison between Different Seasons .....	44
15. “Strong Events” Time Period .....	45
16. SSH Comparison between “Strong Events” and “Weak Events” .....	46
15. “Strong Events” Time Period .....	45
16. SSH Comparison between “Strong Events” and “Weak Events” .....	46

## ABSTRACT

The Navy Coastal Ocean Model (NCOM) has been used to evaluate the suitability of different wind fields for forcing realistic ocean circulation in a coastal ocean model. Of the three wind fields evaluated, one is obtained from a Numerical Weather Prediction (NWP) model: ETA; two others are derived from satellite scatterometer observations: QSCAT and HYBRID. Differences are observed in the characteristics of each of these fields. Through their use with the NCOM simulations, the effects of these differences on simulation of the coastal ocean circulation are revealed.



## 1. INTRODUCTION

Today, 1.2 billion of the world's population lives near the sea [Ncholls, 2002]. As a result, coastal ocean studies and in particular, coastal ocean modeling, is a rapidly developing area of research in modern oceanography. This work investigates how to simulate the dynamics and processes that govern the coastal oceans' behavior: suitable ocean models and external forcings must be employed. Of the different forcings applied to the ocean, wind stress is perhaps the most essential to the understanding of coastal processes. Herein, a series of experiments are conducted to demonstrate this using a high resolution coastal ocean model and three suitable wind forcing fields.

The success of any ocean model is severely limited by the fidelity of the surface heat fluxes and surface stress fields. Often, significant atmospheric changes can occur over short scales of space and time, particularly in coastal regions, where tropical storms and atmospheric fronts have a significant impact on the ocean's behavior. Oceanic variability on the continental shelf is closely tied to the temporal and spatial variability of local atmospheric forcing [Bamgartner *et al.*, 1999]. Fronts, internal waves, upwelling and mixing processes: in short most of the phenomena of interest to the coastal atmospheric forcing [Bamgartner *et al.*, 1999]. Fronts, internal waves, upwelling and mixing processes: in short most of the phenomena of interest to the coastal oceanographer, are all strongly influenced by local and remote winds.

The West Florida Shelf (WFS,  $15.55^{\circ}N - 31.50^{\circ}N$ ,  $80.60^{\circ}W - 98.15^{\circ}W$ ) (Figure 8) is chosen as the test area with these considerations in mind. The WFS is amongst the broadest continental shelves in North America [Li *et al.*, 1999]. Its inner shelf has an average width of 150 km, making it relatively distinct from its associated shelf break region. In comparison with other continental shelf locations, the WFS is relatively insulated from major ocean circulation currents. Occasionally, near the narrower regions of the shelf and in the external part of the shelf, large intrusions of Loop Current water can penetrate the inner shelf, dominating local circulation over time intervals of two to three weeks [Boicourt *et al.*, 1998]. However, the primary variability of circulation across the WFS arises from wind stress fluctuations [Weisberg *et al.*, 2001, Boicourt *et al.*, 1998]. Previous works have further noted that the WFS produces a sea level response to wind stress stronger than that on the Oregon Coast [Marmorino, 1983, Cragg *et al.*, 1983].

Three different wind forcing fields, which are considered suitable for reproducing the variability of the local atmosphere, are evaluated in this study. The first of these is surface winds obtained from NOAA's medium-range Eta-29 weather model. Previous studies have examined the suitability of the Eta-29 and other weather models to force coastal ocean models in regions like the Middle Atlantic Bight [Bamgartner and Anderson, 1999] with some favorable results. For the remaining two wind fields, observations made by the National Aeronautics and Space Administration's (NASA's) SeaWinds scatterometer are used to construct forcing fields to force the model. Several observations made by the National Aeronautics and Space Administration's (NASA's) SeaWinds scatterometer are used to construct forcing fields to force the model. Several studies have demonstrated that satellite scatterometers, which provide relatively high resolution measurements of ocean surface winds, are also quite suitable for the same task

[*Milliff et al.*, 1999; *Grima et al.*, 1999; *Verschell et al.*, 1999; *Hackert et al.*, 2001]. The second wind field is based solely on objectively gridded scatterometer observations. The third wind field, a hybrid field, is produced with scatterometer observations blended with a background field taken from the Eta-29 analysis.

The Navy Coastal Ocean Model (NCOM) is chosen for use in this study for its high resolution and the robust physics it incorporates [*Martin et al.*, 2000]. It is a recently developed coastal ocean model that possesses a number of adaptable features including a unique hybrid-vertical coordinate system, which makes it well suited for simulating ocean processes in the continental shelf and shelf break regions.

Through the examination of these three different wind fields and a corresponding study of their impact on the ocean model's performance, the usefulness of satellite derived wind fields and numerical weather prediction model wind fields for forcing coastal ocean models is explored. Section 2 presents the wind fields in full detail, as well as the in situ data obtained for this study. Section 3 describes the NCOM model and the configuration of the wind forcing experiments that are conducted. Results from these experiments as well as a study of the wind types' variability appear in section 4. A discussion of these results and pertinent conclusions are given in section 5.

## 2. DATA SETS

A series of individual experiments are conducted to evaluate the influence of three separate wind forcing fields on a coastal ocean model's performance. These three wind forcing fields are discussed in detail below. Descriptions of in situ for validation as well as the resulting ocean model output are also detailed. Surface wind stresses based on the different wind fields are compared, rather than wind speed. Gridded scatterometer data is analyzed as pseudostress and calibrated to a reference height of 10 m, the details of which are introduced in 2.2. A bulk aerodynamic method is used to determine wind stress  $\vec{\tau}$ :

$$\vec{\tau} = \rho C_d \vec{u}_{10} |\vec{u}_{10}|$$

where  $\vec{u}_{10}$  is the wind vector at 10 m and  $u_{10}$ ,  $v_{10}$  are the zonal and meridional components of the wind vector respectively,  $\rho = 1.2 \text{ kg} \cdot \text{m}^{-3}$  is the density of air,  $C_d$  is the drag coefficient [Large *et al.*, 1995] and is determined by

$$C_d = 0.001 (2.7 |\vec{u}_{10}|^{-1} + 0.142 + 0.0764 |\vec{u}_{10}|)$$

This wind dependent function  $C_d$  is used through this study

$$C_d = 0.001 (2.7 |\vec{u}_{10}|^{-1} + 0.142 + 0.0764 |\vec{u}_{10}|)$$

This wind dependent function  $C_d$  is used through this study.

## 2.1 Eta-29 Winds

The Eta model is an established medium-range numerical weather prediction model developed by the National Center for Environmental Prediction (NCEP). Currently, several different versions of the Eta model serve in operation throughout North America. Eta-29, a model variant, is run twice daily by NCEP on a rotated longitude/latitude semistaggered Arakawa E grid with 50 levels in the vertical domain [Black, 1994] as well as a 29-km horizontal resolution. The Eta-29 or MesoETA as it is often called, includes 10-m wind vectors in both its analysis and forecast fields. For experimental use here, these 10m winds are extracted from the 0Z and 12Z forecast field, which will be referred to as ETA later.

## 2.2 Wind Stress from SeaWinds Scatterometer Winds and Scatterometer/Eta Hybrid

Scatterometers are active microwave instruments capable of determining wind vectors over the ocean surface. NASA's SeaWinds scatterometer, is carried onboard the sun-synchronous, polar orbiting satellite, QuikSCAT (QSCAT) launched in July, 1999. Typically, SeaWinds relays wind vectors from 93% of the world's ice-free oceans in a period of 24 hours [Spencer *et al.*, 1996, Bourassa *et al.*, 2002]. This scatterometer data  
Typically, SeaWinds relays wind vectors from 93% of the world's ice-free oceans in a period of 24 hours [Spencer *et al.*, 1996, Bourassa *et al.*, 2002]. This scatterometer data however, has an inhomogeneous distribution due to the satellite's orbital motion. For this reason, a variational method is employed to produce gridded pseudostress fields derived

from the SeaWinds observations. These pseudostress values are then used to determine wind stress and force the ocean model.

The zonal ( $\tau_x$ ) and meridional ( $\tau_y$ ) components of the wind stress are:

$$\tau_x = \rho C_D P_x \text{ and } \tau_y = \rho C_D P_y, \quad (1)$$

where  $\rho$  is the density of air, and  $C_D$  is the drag coefficient. The zonal ( $P_x$ ) and meridional ( $P_y$ ) components of the pseudostress are defined as:

$$P_x = u |\vec{u}| \text{ and } P_y = v |\vec{u}|, \quad (2)$$

where  $|\vec{u}|$  is the scalar wind speed, and  $u$  and  $v$  are the zonal and meridional components of the wind vector as above.

Pseudostress fields for both gridded wind fields which will be called as QSCAT and HYBRID fields are determined through variational approach adapted from [Pegion, et al., 2000] which involves the minimization of a cost function, ( $f$ ), constructed of three weighted terms:

$$f = \sum_{i,j} \left\{ \beta_a \sigma_{obs}^{-2} \left[ (P_x - P_{x_o})^2 - (P_y - P_{y_o})^2 \right] + \beta_d L^4 \left[ \left[ \nabla^2 (P_x - P_{x_{bg}})^2 \right] + \left[ \nabla^2 (P_y - P_{y_{bg}})^2 \right] \right] + \beta_e L^2 \left[ \hat{k} \bullet \nabla \times (\bar{P} - \bar{P}_{bg})^2 \right] \right\} \quad (3)$$

where the betas are weights, the  $i, j$  subscripts for geographical position have been

where the betas are weights, the  $i, j$  subscripts for geographical position have been

dropped, the pseudostress ( $P_x, P_y$ ) without additional subscripts is the solution field, the

'o' subscript indicates observations, the subscript 'bg' indicate the background field,  $\sigma$  is

the uncertainty in a grid cell's observed wind component, and  $L$  is a length scale of the latitudinal grid spacing that make the functional dimensionally sound. The  $\beta_a$  term of  $f$  scales the misfits to the observational values. The  $\beta_d$  term scales regularization relative to a chosen background field. The last term minimizes the misfit of the curl of the pseudostress, relative to the same background field. Each of these constraints is multiplied by a weight ( $\beta_a, \beta_d, \beta_e$ ). In practice, the equation is simplified by dividing by  $\beta_a$ , resulting in only two weights (in other words,  $\beta_a$  is set to unity). These weights are determined through cross validation [Pegion *et al.*, 2000] resulting in  $\beta_d = 0.01$  and  $\beta_e = 0.02$  with negligible seasonal variation.

These weights are fixed to the same value for the construction of the QSCAT and HYBRID data sets. The differences between the QSCAT and HYBRID fields are due to the different background fields. For construction of the QSCAT only gridded data set, the background pseudostress field is generated after passing QSCAT wind observations through a Gaussian filter in time and space and standard deviation of 6 hours and  $2^\circ$ . For the HYBRID data set, this background is obtained from the 0Z and 12Z analysis of the Eta-29. While the scatterometer instrument has a gridded spacing of 25 km, both of the gridded fields evaluated in this experiment are produced on a  $0.5^\circ \times 0.5^\circ$  grid.

### 2.3 NDBC Buoy Winds

#### 2.3 NDBC BUOY WINDS

Winds from the three different fields discussed above are compared to in situ observations made by a National Data Buoy Center (NDBC) buoy. The NDBC maintains an extensive network of buoys and associated observational stations throughout the

coastal waters of the U.S. These stations routinely provide observations of ocean variables as well as standard meteorological data, including wind speed and direction. For the analysis conducted in this study, data from buoy 42036 is used. This buoy is moored in the Northwest region of the WFS, at 28.51°N, 84.51°W (Figure 1 and Figure 8). The measurements of wind speed and direction were made using a conventional anemometer mounted 5m above the base of the buoy (ocean surface). Both wind speed and wind direction measurements were averaged over an eight-minute period and reported hourly. [National Data Buoy Center, 2002, available at <http://ndbc.noaa.gov/measdes.shtml>]

In situ 5 m buoy observations are corrected to 10 m using the formula:

$$|\vec{u}_{10}| = 1.075 |\vec{u}_5|$$

where  $|\vec{u}_5|$  is the wind magnitude at 5 m,  $|\vec{u}_{10}|$  is the wind magnitude at 10 m, the coefficient 1.075 is calculated from a power law relationship and it is also consistent with the BVW [Bourassa *et al.*, 1999] height adjustment for a neutral atmospheric stratification.

#### 2.4 In Situ Sea Surface Height (SSH) Observations

Sea Surface Height (SSH) observations used in this study are obtained from the Center for Operational Oceanographic Products and Services (CO-OPS). CO-OPS collects, analyzes and distributes historical and real-time observations and predictions of ~~coastal oceanographic data~~ collects, analyzes and distributes historical and real-time observations and predictions of water levels, coastal currents and other meteorological and oceanographic data as part of an integrated National Ocean Service program which functions in conjunction with the National Weather Service, which are both administered by the National Ocean and



Atmospheric Agency. [*Center for Operational Oceanographic Products and Services, NOAA, 2002, <http://co-ops.nos.noaa.gov/>* ]

The primary water level measurement was obtained from a downward looking acoustic sensor. Measurements were taken at 6-minute intervals with each measurement consisting of a set of 181 one-second interval water level samples centered on each tenth of an hour. The 181 samples were averaged, a three standard deviation outlier rejection test applied, and the mean and standard deviation recalculated and reported along with the number outliers. The reported measurements had 0.01 ft resolution. [*Center for Operational Oceanographic Products and Services, NOAA, 2002*]

SSH data are obtained from the stations at Apalachicola (APA,  $29.73^{\circ}N$  ,  $84.98^{\circ}W$  ), Cedar Key (CDK,  $29.14^{\circ}N$  ,  $83.03^{\circ}W$  ), Clearwater Beach (CWB:  $27.98^{\circ}N,82.83^{\circ}W$  ) and Naples (NPL  $26.13^{\circ}N,81.81^{\circ}W$  ) from north to south, west to east along the WFS.

### 3. MODEL DESCRIPTION AND WIND FORCING EXPERIMENTS

#### 3.1 NCOM Model Description

The Navy Coastal Ocean Model (NCOM) is used in this study to evaluate the influence of different wind forcing fields on coastal ocean simulations. The complete NCOM description is presented in detail by Martin [2000]. Still, while the NCOM is relatively a new model, it is based primarily on two ocean models, the Sigma-Z model (SZM) developed by [Martin *et al.*, 1998], and the Princeton Ocean Model (POM) developed by [Blumberg and Mellor, 1983, 1987]. The basic physics and numerics of the NCOM originated from the POM. Higher order numerical schemes were later incorporated. A hybrid sigma-z-level vertical coordinate system is added as in the SZM to make the NCOM better adapted to studying phenomena in coastal waters.

Like POM and the SZM, the NCOM is based on primitive equations of motion. It employs a free surface at the atmospheric-ocean boundary, and assumes hydrostatic, incompressible, and Bussinesq approximations. Temperature, salinity, three dimensional velocity, and sea-surface height are prognostic variables of the model. The model equations are solved on an Arakawa C grid with a semi-implicit time integration scheme and a third order upwind differencing method for advection [Holland *et al.*, 1997].

Among the most unique aspects of the NCOM is its hybrid vertical coordinate system composed of both sigma and z-level layers. The versatility of this structure allows for improved simulations of ocean circulation on the continental shelf and more accurate simulations over the entire shelf (Figure 2). This coordinate system may be configured to best suit varying shelf topographies. As can be seen, the use of sigma layers provides for terrain following layers over the very gradually sloping shelf plateau, thereby allowing the model to more accurately reproduce the shallow water dynamics. Along the shelf break however, where steeply sloping topography arises, use of sigma coordinates proves problematic in the determination of horizontal gradients. Transitioning to Z- levels in such regions eliminates this problem. The use of both vertical coordinate types in the regions of their respective strengths thus allows for a highly accurate simulation of the circulation over the entire shelf region.

The model may be forced by atmospheric pressure, tidal potential, river and freshwater runoff, surface heat fluxes, salt fluxes and inflow at open boundaries.

### 3.2 Numerical Experiments

The above description relates the versatility of the NCOM and its unique ability to be configured for almost any particular interest in coastal studies. Here, the configuration of the NCOM is such to facilitate examination of the coastal ocean's response to different wind forcing regimes. (wind driven phenomena scale). In the experiments conducted, the resolution of the model's horizontal grid was set to  $\frac{1}{20}^\circ$  (roughly equivalent to 5 km) with a time step fixed to 400 seconds. Each simulation employs a vertical grid using 20

evenly spaced sigma layers above 100 m and 20 Z-level layers below 100 m. The depths of the z-levels are chosen so that the first one below 100 m is spaced at 5 m, and the remaining stretched logarithmically to the bottom with a maximum depth of 4000 m.

While the region studied for these experiments is confined to the WFS. The domain for each model simulation encompasses the entire Gulf of Mexico ( $15.55^{\circ}N - 31.50^{\circ}N$ ,  $98.15^{\circ}W - 80.60^{\circ}W$ ), with open boundaries in the Caribbean Sea to the Southeast as well as the Florida Straits to the East. Inflow in the Caribbean forces a Yucatan Strait transport of roughly 30 Sv.

Data derived from  $0.5^{\circ} \times 0.5^{\circ}$  analyzed COADS monthly climatology fields [DaSilva, 1994] are used to calculate surface fluxes of heat (latent heat flux, sensible heat flux and radiative heat fluxes penetrating the ocean's surface with a Jerlov type extinction profile) for all simulations. A spatially uniform, temporally constant surface salt flux is consistent with evaporating the same amount of fresh water input by the 30 principle rivers from stations both in the United States and Mexico. Sea surface temperature is relaxed to monthly climatology (through a heat flux correction) with a time scale proportional to the mix layer depth, that is,  $T = \frac{1}{k} H$ , where  $k = 1 \text{ m} \cdot \text{day}^{-1}$ .

The separate model simulations conducted to evaluate the different forcing fields are conducted for a period of nearly eighteen months, from July, 1999 to December, 2000. This period begins after a five-year span during which the NCOM is initialized at rest with temperature and salinity data taken from the World Ocean Analysis [WOA, 1994] and run with the climatological forcing.

For the individual wind forcing experiments, wind stress is generated from the 3 individual wind fields described in section 2. For each wind field, a separate simulation is

made. For all simulations, wind stress is interpolated to the model grid using bicubic splines interpolated linearly in time between 12 hourly records.

## 4. RESULTS

Results from the experiments described in section 3 are analyzed in two phases. The first phase of this analysis consists of an examination of the intrinsic behavior of the ETA, QSCAT and HYBRID winds and their comparison with in situ observations on the WFS. In the second phase of analysis, the influence of each wind field behavior on the NCOM's ocean simulations is investigated. In particular, coastal sea surface height (SSH) is examined as a variable that reflects the influence of the wind fields on the ocean model's performance.

### 4.1 Wind Variability

An evaluation of each wind field is made by comparing the wind vectors at one location with in situ observations. This evaluation is conducted for the approximately eighteen-month time period of the study. This serves as a more or less "quick look" of the variability, and reveals many interesting inherent characteristics of each of the wind fields studied.

variability, and reveals many interesting inherent characteristics of each of the wind fields studied.

Time series of the wind fields (Figure 3) at the NDBC buoy location qualitatively expose many of the intrinsic characteristics of each wind data sets. It can be seen that the

ETA winds are generally in the same direction as that observed by the buoy. However, the magnitude of the ETA wind stress field is much smaller than that of the observations. This deficiency is especially pronounced during strong atmospheric events, many of which are typically observed in the Gulf of Mexico region.

In contrast, gridded QSCAT wind stress vectors compare more closely in magnitude with the same buoy observations. Unlike the ETA wind stress, QSCAT does noticeably well in duplicating in situ observations of stronger events as well as typical circulation patterns. The HYBRID wind stress field behaves quite similarly to the QSCAT.

While these are general traits observed throughout the period of this study, a more quantitative comparison of the different wind fields can be made by computing the complex correlation of wind stress vectors of the different wind fields with in situ observations. Like its linear counterpart, the complex correlation yields a coefficient whose value relates similarity in different time series patterns [Kundu *et al.*, 1975]. Unlike the linear correlation however, the complex correlation also relates similarities in phase in the form of an average veering angle. Thus, the complex correlation serves as a valuable tool for analyzing the behavior of different sets of vectors (Figure 4a, 4b).

The ETA wind stress field has the highest correlation coefficient value of the three fields evaluated, followed by the QSCAT (value) and HYBRID (value) fields. The ETA model wind fields on average appear more in phase with the buoy observations than either of the scatterometer based fields. It should be noted that NDBC buoys have a propeller-vane anemometer which records measurements once every hour (an 8-min average of the wind speed and a single direction) with accuracies of  $1 \text{ ms}^{-1}$  and  $10^\circ$ , for wind speed and direction respectively [Gilhousen, 1987]. Thus, the average veering

angles, for the scatterometer-derived wind fields are comparable in magnitude to the instrument error.

Wind stress magnitude is important to the behavior of ocean models. Thus, in addition to the complex correlation analysis, time averages of wind stress magnitude are also determined for each of the different wind fields and compared with the buoy observation. The QSCAT and HYBRID forcing fields produce mean wind stresses that are very similar to that measured by the buoy (Figure 4c), with the QSCAT wind stress magnitude 9% lower and the HYBRID wind stress magnitude 4% larger than the buoy wind stress magnitude. Contrastingly, the ETA is the weakest winds of all data sets considered. Its mean wind stress magnitude is less than half of the in situ observations (Figure 4c). The results could be different elsewhere. However, there are three snapshots of the wind fields for the whole GoM from three different wind fields on Sep, 20, 1999, when a tropical storm, Harvey passed by (Figure 5). It is shown that all three wind fields have the similar pattern, with a low pressure center (tropical storm) near the east of GoM or WFS. But it is also obvious that the intensity of the low pressure are different, with ETA wind field the weakest, the HYBRID strongest, QSCAT in the middle. Correspondingly, there are differences in the coastal sea level fluctuations to different wind fields.

The plot of the wind vector time series suggests that there is a pronounced seasonal variability in weather patterns observed over the WFS (Figure 6). It appears that between October and April strong atmospheric events are more frequent in the WFS region. In this variability in weather patterns observed over the WFS (Figure 6). It appears that between October and April strong atmospheric events are more frequent in the WFS region. In this period, which henceforth shall be referred to as the "winter season", the atmosphere is active with the passage of strong cold fronts moving across the WFS. In the period of



May through September however, or “summer season,” more moderate atmospheric activity prevails. Unlike during the winter months, energetic events occur with a considerably reduced frequency and intensity. This season is tempered by weaker winds, with the exception of occasional tropical weather systems that may pass through the region.

Characteristics of the wind products discussed previously are generally applicable to the summer months and winter months when treated separately (Figure 7). The QSCAT and HYBRID fields still have similar mean magnitudes as the buoy winds, and the ETA wind stress remains approximately one half that measured by the buoy. However, the mean wind stress is significantly greater during the winter months so it is at this time that one expected the Eta model underestimation of the wind stresses to have the most profound impact on the ocean model solution. This will be examined in section 4.2.2.

## **4.2 Sea Surface Height Response to Different Wind Fields Forcing**

### **4.2.1 General**

A separate model simulation is conducted for each different wind forcing field. These will be referred to as NCOM/ETA, NCOM/QSCAT, and NCOM/HYBRID respectively. From these individual trials, the model output is compared with the in situ data along the WFS. Variability in coastal sea level is dominated by local wind forcing on the shelf in  
From these individual trials, the model output is compared with the in situ data along the WFS. Variability in coastal sea level is dominated by local wind forcing on the shelf in  
GoM. For this reason, the sea surface height field (SSH) of the model results is of particular interest in this analysis.

Four observational locations are chosen to study the variability in simulated sea surface height as a function of the different wind forcing fields. These stations are located along the WFS at Apalachicola (APA), Cedar Key (CDK), Clearwater Beach (CWB), and Naples (NPL) (Figure 8). Simulated records are obtained from the model grid points nearest to these locations and comparisons are made between simulated and observed SSH. All of the simulations are conducted without the presence of tides or the contribution of atmospheric pressure in the model. As a result, the in situ observations are detided following the method of *Foreman* [1996].

First, in a comparative study of the SSH variability, the SSH anomaly for each simulation as well as observations is examined (Figure 9). These results exhibit analogous variability to that of the wind fields as discussed earlier (Figure 3). Simulated SSH variability from NCOM/ETA appears significantly smaller in magnitude than that generated by the NCOM/QSCAT and NCOM/HYBRID, as well as observation. During several strong events in the fall of 1999 and the fall of 2000, this discrepancy between the ETA trial and the other values appears largest, just as in the original wind fields themselves. From a snapshot of the SSH fields on WFS during the time when tropical storm Harvey passed by GoM, the difference between simulated SSH from different model runs are very clear (Figure 10): there is no sign of upwelling due to the Harvey arrival in NCOM/ETA simulation results; there is very obvious upwelling in NCOM/QSCAT model runs, with much stronger current flowing toward the coast where upwelling occurs; in NCOM/HYBRID, upwelling appears with larger amplitude and area.

Linear correlations of simulated SSH and observational data are computed over the entire time period at each of the four stations (Figure 11a). It is apparent that the correlations of SSH from the NCOM/QSCAT and NCOM/HYBRID with the in situ data are consistently higher at each station than from the NCOM/ETA. Calculation of root-mean-square error (RMSE) scaled by the standard deviation of the observed SSH at each station (Figure 11b) reveals similar behavior. At each station, the scaled RMSE value of the NCOM/ETA simulations is much larger than that of the NCOM/QSCAT and NCOM/HYBRID model runs.

Since the model simulations are conducted without considering the contribution of atmospheric pressure, an inverse barometer calculation is made to adjust the simulated SSH at two stations. The resulting correlation coefficients and scaled RMSEs are improved at each station (Figures 12, 13, Table 1a and 1b). It is interesting that the benefit of the added atmospheric pressure contribution significantly improves results of the NCOM/ETA model run.

#### **4.2.2 Seasonal Sea Level Response on the WFS**

In continental shelf waters, large sea level fluctuations typically correspond to energetic atmospheric forcing. Indeed, there appears to be a very similar seasonal fluctuation in the frequency of energetic ocean events in the WFS region to that observed in the previous analysis of the regional winds. Characteristics of the previously fluctuation in the frequency of energetic ocean events in the WFS region to that observed in the previous analysis of the regional winds. Characteristics of the previously determined seasons, winter and summer, hold true for the ocean variables examined here. In response to strong atmospheric forcing between October and April, larger amplitude

sea level fluctuations are more frequently observed on the WFS than during the summer months of May through September.

Correlation coefficients and RMSEs (scaled by the standard deviation of the observed SSH during each season) are recalculated for the two previously established seasons (Figure 14a –14h). The NCOM/ETA results show little change from season to season. That is, the errors increase as the variance (STD) of the sea level fluctuations increases. The NCOM/QSCAT and NCOM/HYBRID results however, show markedly higher sea level correlation with observations during the winter season than during the summer. The RMSEs scaled by the seasonal standard deviation of observed sea level also show improvement during the winter season. These results suggest that the greatest enhancement of the NCOM simulations performance by the two scatterometer derived wind forcing fields, QSCAT and HYBRID, occurred during the more energetic wind forcing of the winter season. It is also obvious that during the two time periods, the correlation coefficients between simulated SSH from NCOM/QSCAT, NCOM/HYBRID and observed SSH are always nearly equal to or higher than that from NCOM/ETA. The scaled RMSEs from NCOM/QSCAT and NCOM/HYBRID are similarly nearly equal or smaller than that from NCOM/ETA. While the analysis of the wind variability suggested that the ETA should be quite suitable for forcing an ocean model considering its good correlation with observation, serious doubts of this appear in the examination of the NCOM/ETA simulation results.

This analysis suggests that it may be useful to more carefully focus interest on the NCOM/ETA simulation results.

This analysis suggests that it may be useful to more carefully focus interest on the model response during large amplitude sea level events. The sea level time series are objectively decomposed into two parts. The first part is obtained by taking seven day

windows centered around observed sea-level anomalies whose magnitude is greater than two standard deviations computed from the complete record. This part is designated as a 'strong events' subset of the record, and composed mostly of events occurring during the winter season discussed above. Only few events in the summer season, including three tropical systems, are included in the strong event subset. This subset includes about 20% of the full time record. The second part comprises the remaining sea level record. This part, deemed the 'weak events' subset, contains only weak or moderate sea level fluctuations, most of which are observed during the summer season (Figure 15). The RMSEs scaled by the standard deviation of the observed SSH from strong/weak events are calculated to study the effect of the differences of the different wind stress forcings on the ocean during these energetic fluctuations.

It is apparent that the SSH from NCOM/ETA simulation during strong ocean events has by far the largest error of the three simulations considered (Figures 16i, 16j, 16k and 16l). Results from the NCOM/QSCAT and NCOM/HYBRID numerical experiments have much smaller errors and are very similar to each other. When the simulated SSH is considered for periods excluding strong events (Figures 16e, 16f, 16g and 16h), there is little difference in RMSEs values for either NCOM/ETA, NCOM/QSCAT or NCOM/HYBRID runs during this subset of the period studied.

The RMSEs calculated for the whole study period reveal a similar pattern to that observed when scrutinizing periods with strong events alone. This shows that the influence of the strong events is substantial over the period studied. These events play a significant role in the overall wind driven variability of the WFS sea surface. They also

place a strict requirement that wind fields be chosen such that they suitably force ocean models for these periods of time.

Thus it is noted that there are great differences between the ocean model solution during strong events for the model runs forced by the ETA winds versus the scatterometer-derived wind fields and relatively little difference for periods when such strong events are absent. It is evident that the pattern of the RMSE observed for strong events impacts the RMSE determine for the entire period of study (Figures 16a-d and 16i-1). Also, as in the detailed examination of strong ocean events alone, the RMSE is significantly higher for the NCOM/ETA simulation, and, for the QSCAT and HYBRID simulations, nearly identical.

From this analysis it is clear that the representation of strong atmospheric events in the wind stress field has a great influence on the ability of the model to correctly simulate coastal sea level. The ability of the QSCAT and HYBRID wind fields to accurately capture strong events in the atmosphere translates into a more realistic rendering of the coastal ocean circulation in the model. For the ETA wind field, the inability of the weather model to represent accurately the energetic weather over the ocean equates to a poorer simulation of the ocean's response in the model.

## 5. CONCLUSIONS

The NCOM has been used to evaluate the suitability of different wind fields for forcing realistic ocean circulation in a coastal ocean model. Of the three wind fields evaluated, one is obtained from a Numerical Weather Prediction (NWP) model, and two others are derived from satellite scatterometer observations. Differences are observed in the characteristics of each of these fields. Through their use with the NCOM simulations, the effects of these differences on simulation of the coastal ocean circulation are revealed.

The Eta-29 is a high resolution weather model and has been considered a very good candidate for coastal ocean modeling applications in North America. However, results of this study strongly suggest that wind fields produced by the Eta should be used with caution. At first glance, the Eta-29 exhibits a high correlation with the local wind stress variability. Through comparison of wind stress derived from in situ observations though, it is apparent that the Eta-29 seriously underestimates the intensity of the local wind stress. This weakness in wind stress magnitude produces a much weaker ocean response in the NCOM simulation. This is clearly evident in the examination of sea-level variability.

in the NCOM simulation. This is clearly evident in the examination of sea-level variability.

Very few previous studies have used satellite scatterometer winds to provide surface forcing for ocean models and even fewer (if any) for coastal ocean models. This is in

large part due to the incomplete coverage of scatterometer observations in space and time. However, it is shown here that this limitation may be overcome and, when properly used, these satellite surface winds can be quite useful for coastal ocean simulations. Scatterometers provide high resolution surface winds over the ocean and offer equal or better accuracy than most conventional marine observations. Here, it is shown that using a variational method, scatterometer winds may be blended with a background field to produce a new set of spatially and temporally complete gridded surface forcing fields. It is useful for forcing ocean models for studying ocean dynamics in coastal regions with high resolution in space and time.

Two such scatterometer-derived fields are evaluated in this study. The QSCAT field is created by after applying the variational method using binned and smoothed scatterometer observations as a background field. The HYBRID field is created using the same method, but with a background derived from the Eta-29 model data. In comparison with in situ observations, the QSCAT and HYBRID fields quite reasonably represent the variability of the wind stress over the WFS. Both wind fields exhibit a high correlation with buoy observations. Unlike the ETA, the consistency of the QSCAT and HYBRID wind stress fields magnitude is maintained during strong atmospheric events. This is proven to be crucial to the corresponding oceanic response simulated by the NCOM.

The NCOM simulations which employ wind stress forcing from the QSCAT and HYBRID fields compare most favorably with in situ observations. Over the entire study time period, the NCOM/QSCAT and NCOM/HYBRID simulations demonstrate the H Y B R I D fields compare most favorably with in situ observations. Over the entire study time period, the NCOM/QSCAT and NCOM/HYBRID simulations demonstrate the highest correlation of sea level variability and the smallest RMSE relative to the observations. In contrast, the NCOM/ETA simulations exhibit the largest RMSE relative



to observation, and a much lower correlation. During periods of strong local wind events, the NCOM/ETA simulations produce much weaker corresponding sea level responses in magnitude than the observed variability. Where a high correlation is observed between the ETA winds and observation, the weakness of the ETA derived wind stress field produces a correspondingly weak correlation between NCOM simulated SSH and that observed in the ocean.

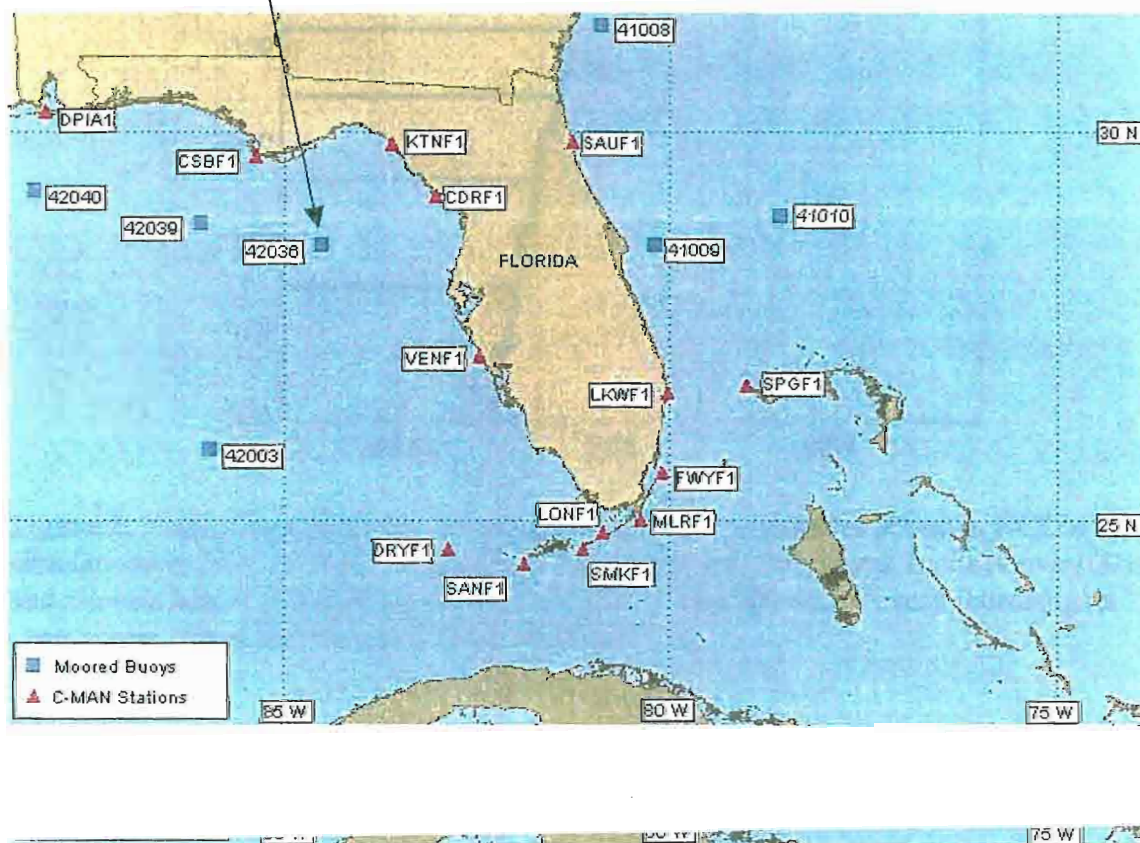
It is evident that the major differences in the ETA, QSCAT, and HYBRID winds arise when the nature of the local wind variability changes seasonally. Observational data examined during the full period of study exhibits a pronounced seasonal variability in the winds and the corresponding SSH. This seasonal variability has an impact on the evaluation of the winds and their influence on the NCOM simulations. During the summer season, tempered by moderate atmospheric activity, the ETA, QSCAT, and HYBRID fields differ less from each other and closely represent the observed winds. For the occasional strong events that are observed in the late summer, significant differences occur between the wind fields, and between the ocean simulation results. In the winter season these differences are most pronounced because many more energetic events occur in this season in the GoM and across the WFS. Both the QSCAT and HYBRID fields seem to excel in these conditions. NCOM/QSCAT and NCOM/HYBRID simulations during the winter perform quite well, with the simulated coastal sea level correlating well with observed energetic ocean sea level fluctuations and relatively low RMSE values relative to in situ observations. NCOM/ETA simulations fail to capture the full magnitude of the same events, with modeled sea level correlating less well and with increased errors to observations.

Thus, in an effort to evaluate different wind fields to be used in coastal ocean modeling, it is found that both of the scatterometer-derived fields are most suitable. The Eta-29 model, while seemingly attractive at first, exhibits serious underestimates of wind stress magnitude compared with observations. This deficiency translates into insufficient momentum flux to the surface of the ocean model, and therefore weaker simulated sea level response. This is most evident during energetic wind-driven events. In contrast, simulations conducted with both scatterometer fields, QSCAT and HYBRID perform very well. Results from both simulations are nearly identical, exhibiting a pronounced skill in reproducing the response of the ocean surface to the local wind.

## Buoy Station Map



**Figure 1.** Station 42036 (28.51 N 84.51W) which is owned and maintained by National Data Buoy Center (NDBC). Site elevation: sea level; Air temp height: 4 m above site elevation; Anemometer height: 5 m above site elevation; Barometer elevation: sea level; Sea temp depth: 0.6 m below site elevation; Water depth: 53.0 m; Watch circle radius: 126 yards.



### NCOM Vertical Coordinate System

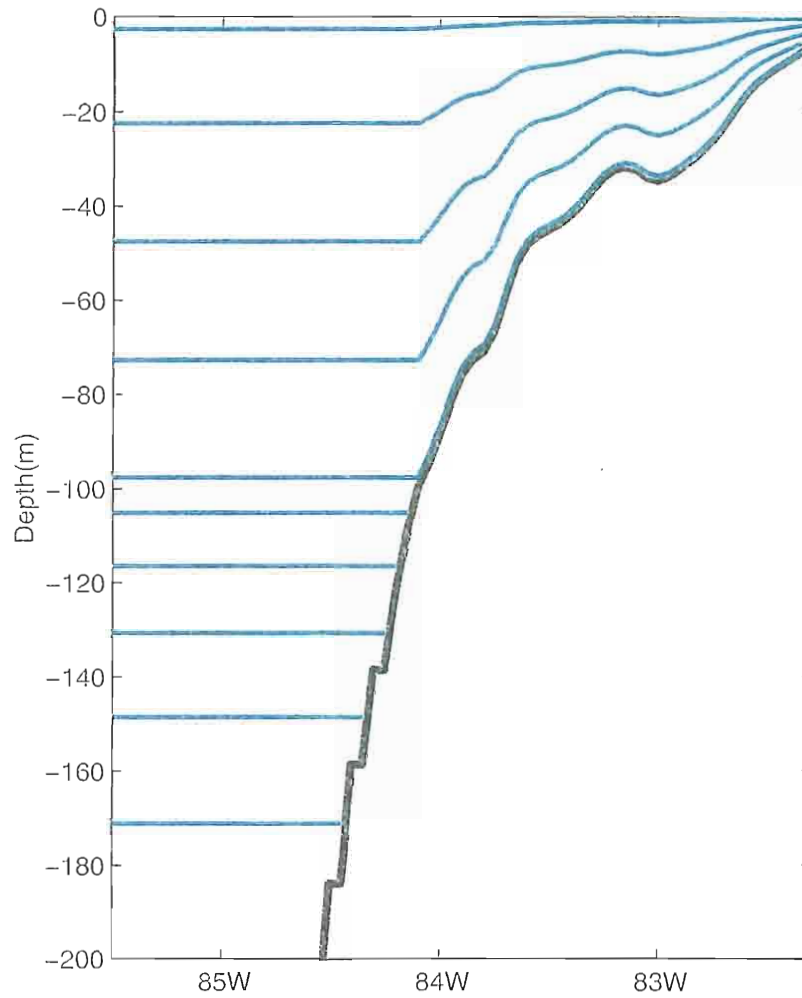


**Figure 2.** Illustration of the way the combined sigma/z-level grid is set up in NCOM simulations at 27 N on West Florida Shelf (above 200 m), with sigma layers above 100 m and z-levels below 100 m (the middle of the grid cell are shown for every fourth sigma layer above 100 m and for every Z level below 100 m).

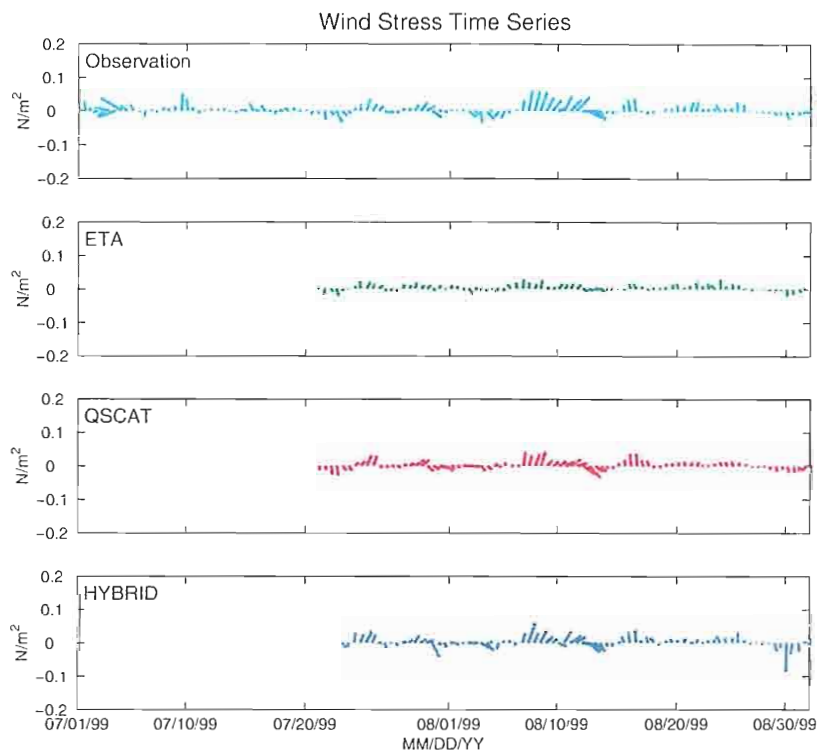


**Figure 3.** Wind stresses from observation (cyan), ETA (green), QSCAT (red) and HYBRID (blue) from July, 1999-Dec, 2000 at  $28.51^\circ$  N,  $84.51^\circ$  W (to be continued).

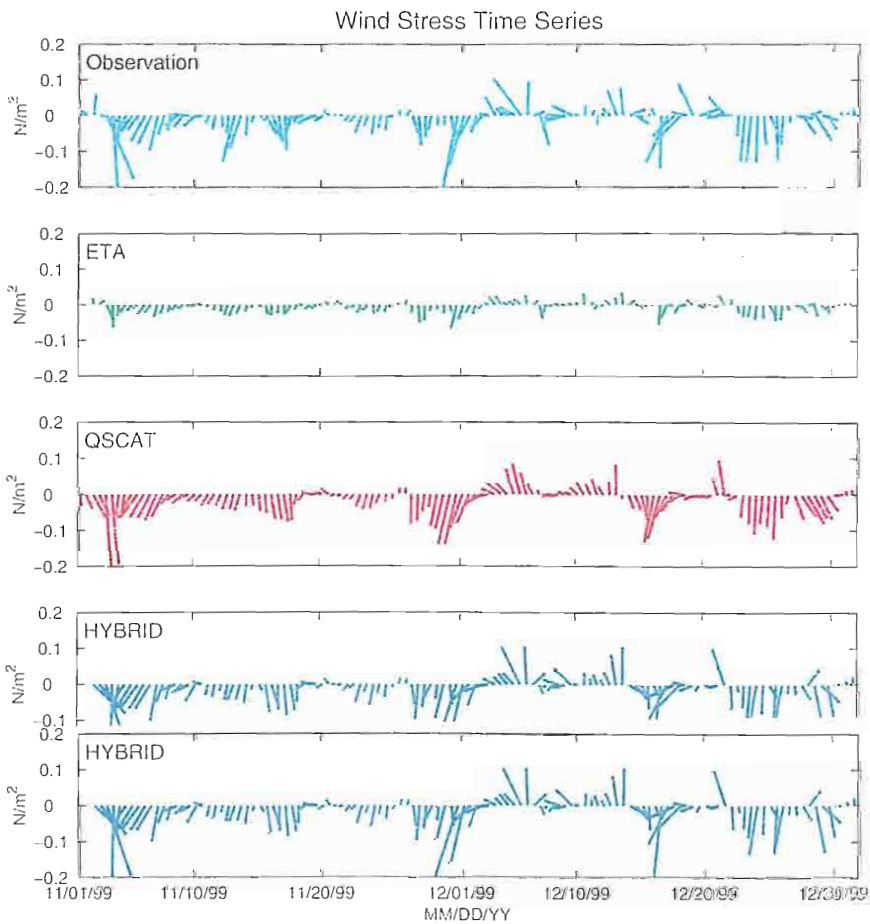
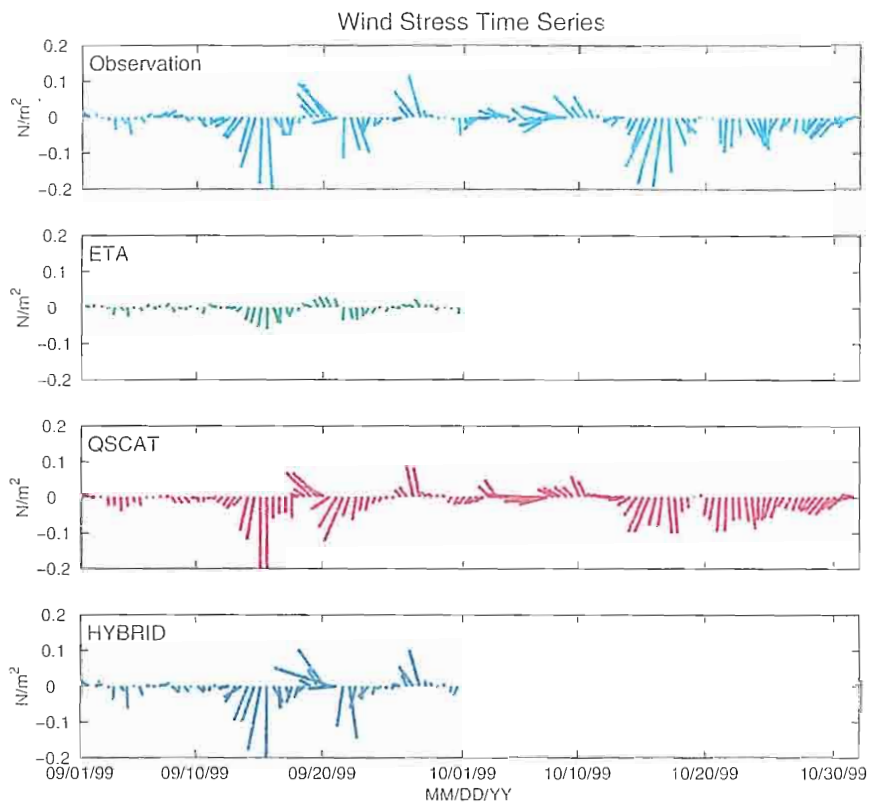


Figure 3. Continued,

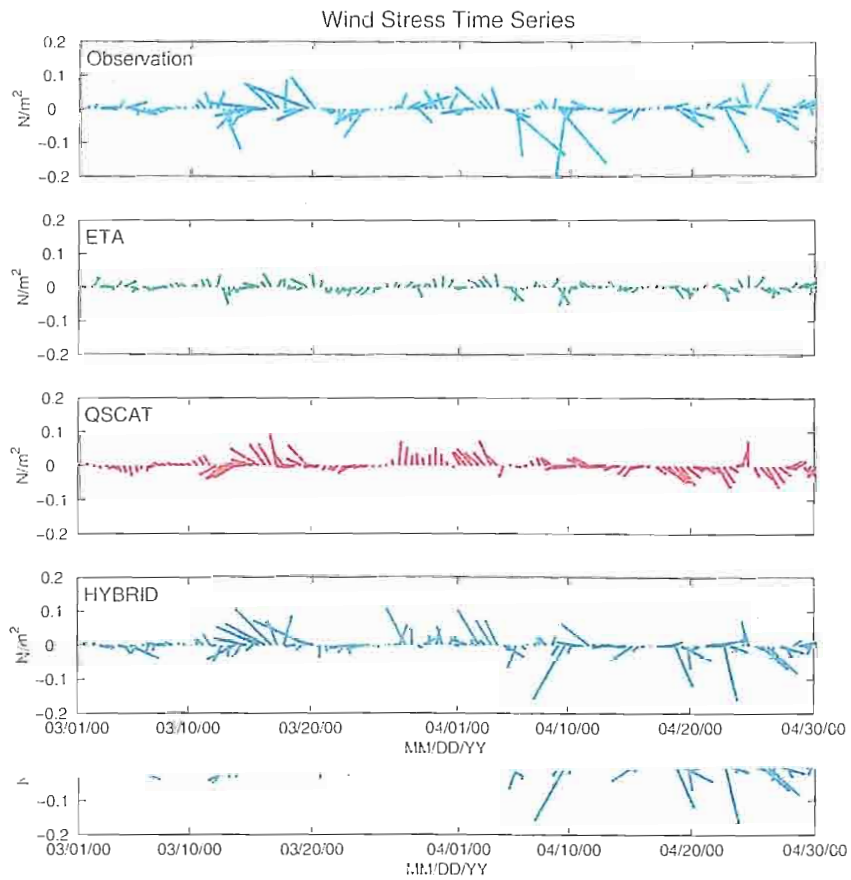
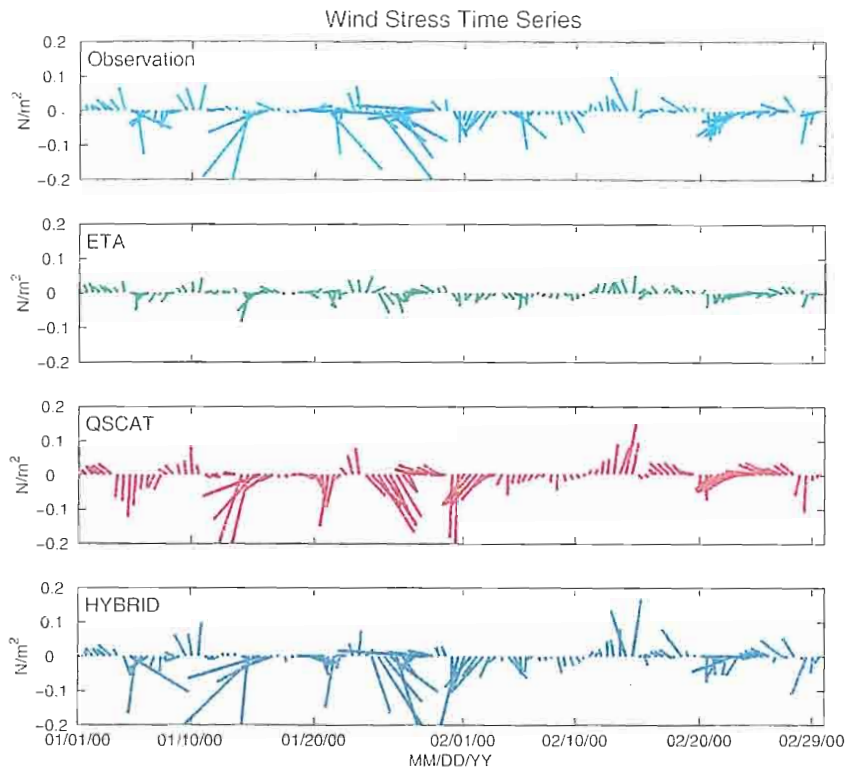


Figure 3. Continued,

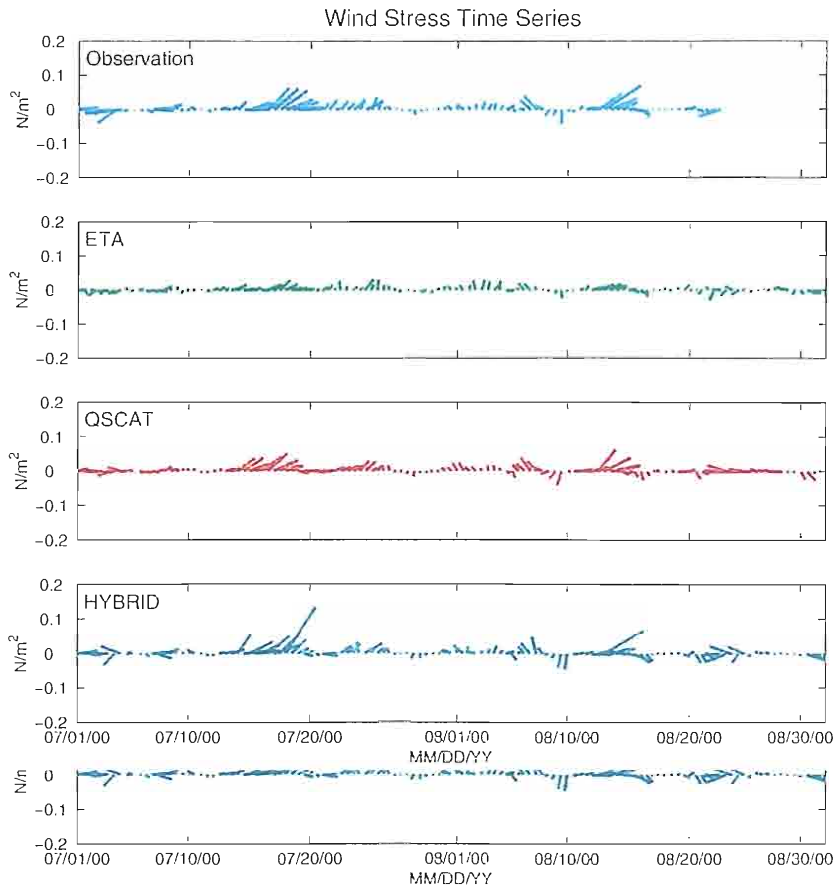
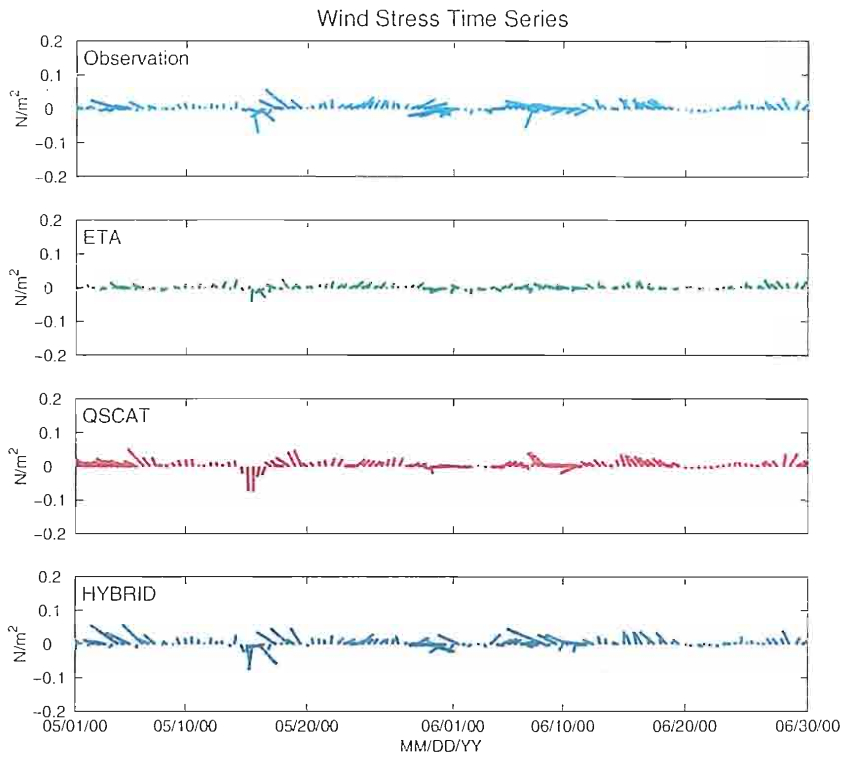


Figure 3. Continued,



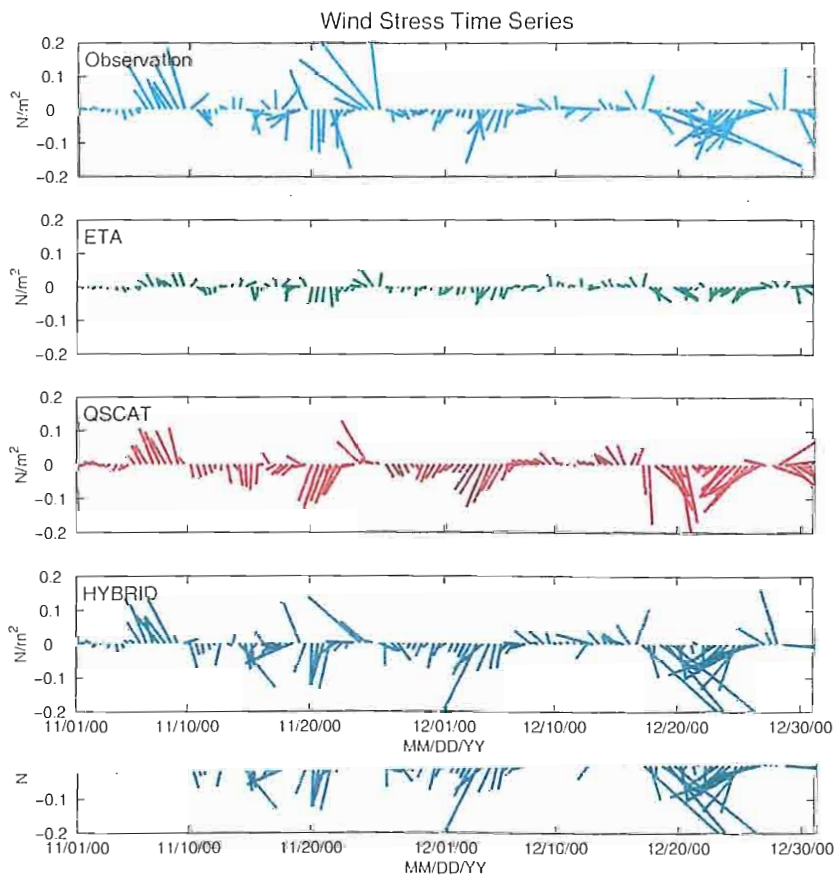
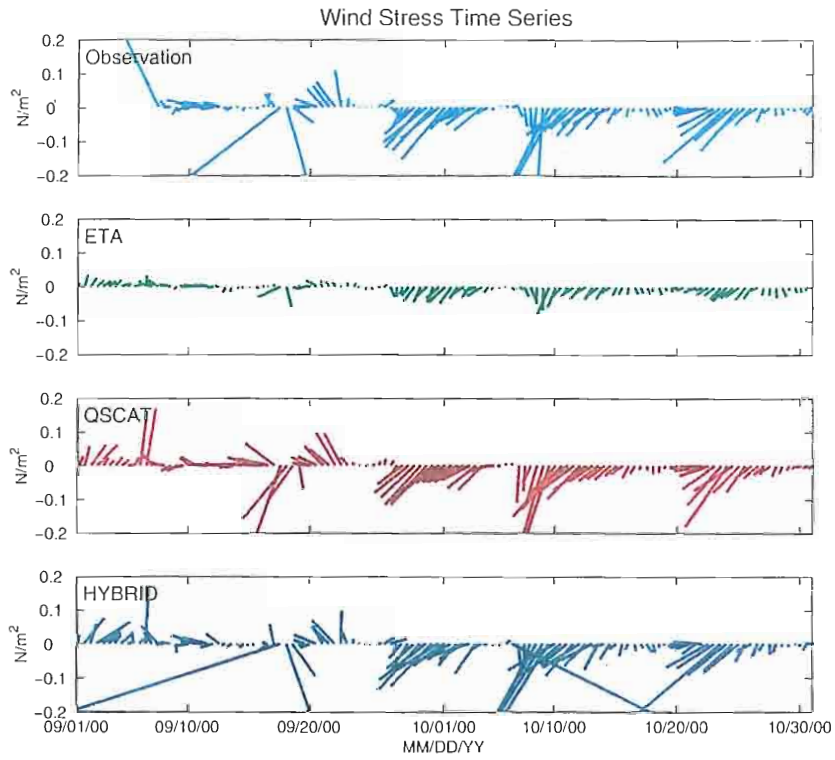
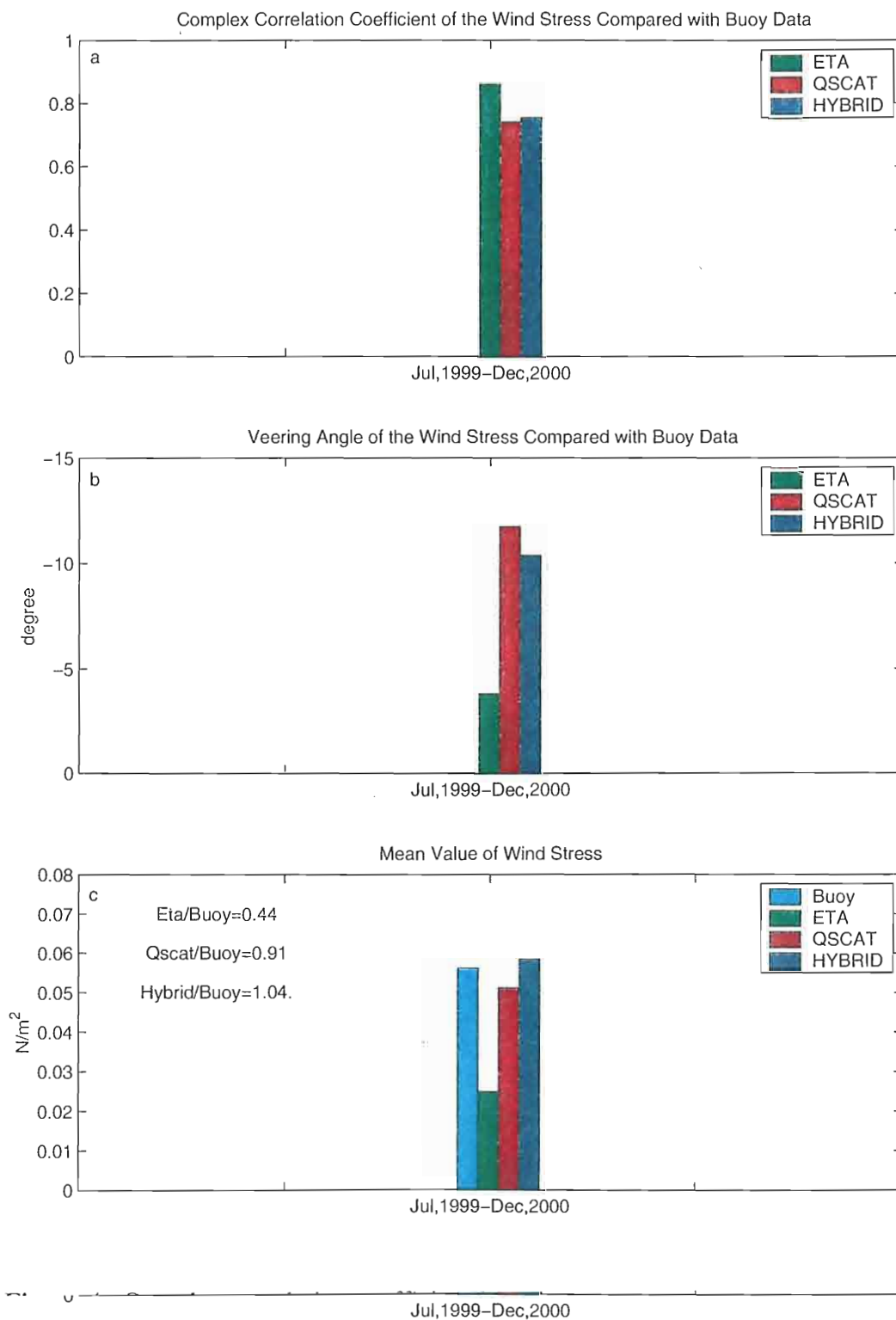


Figure 3. Continued.

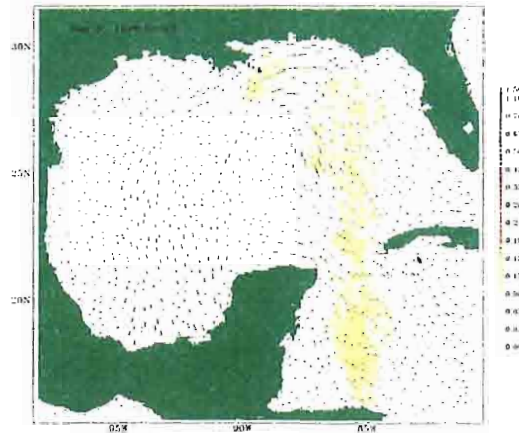
## Wind Stress Comparison between Observation and ETA, QSCAT and HYBRID



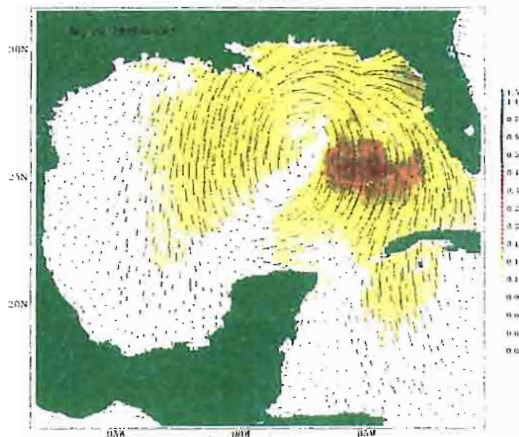
**Figure 4.** Complex correlation coefficient (a), average veering angle (b) and mean value (c) of wind stress from ETA (green), QSCAT (red) and HYBRID (blue) wind fields compared with buoy observation (cyan) from July, 1999–Dec, 2000 at 28.51° N, 84.51° W.

Wind Fields Snapshots from ETA, QSCAT and HYBRID

ETA



QSCAT



HYBRID

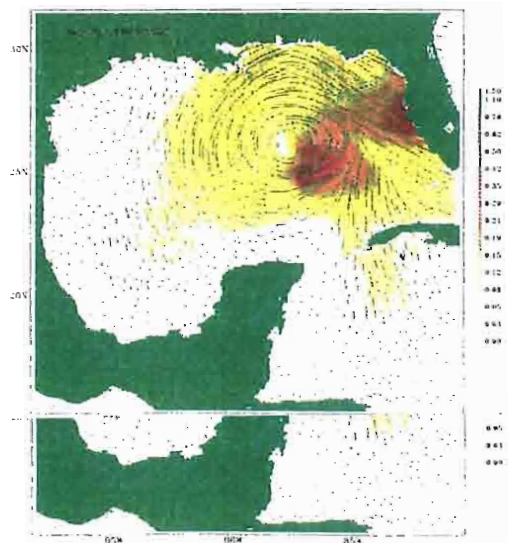


**Figure 5.** Snapshots from the ETA, QSCAT and HYBRID wind fields taken from the entire GoM. These snapshots capture the arrival of tropical storm Harvey on September 20, 1999, 00:00 Z.

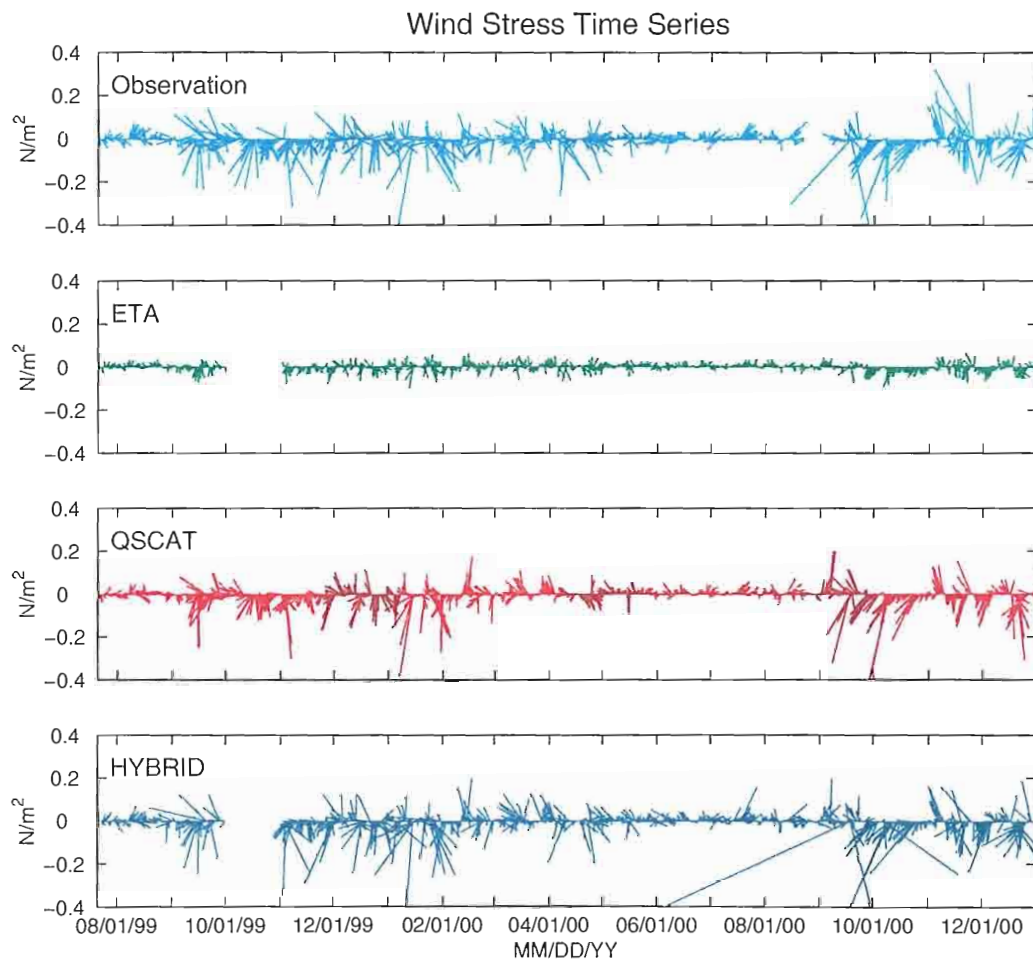


**Figure 6.** Wind stresses from observation (cyan), ETA (green), QSCAT (red) and HYBRID (blue) from July, 1999-Dec, 2000 at  $28.51^\circ \text{ N}$ ,  $84.51^\circ \text{ W}$ .

## Wind Stress Comparison between Different Wind fields During Different Time Periods

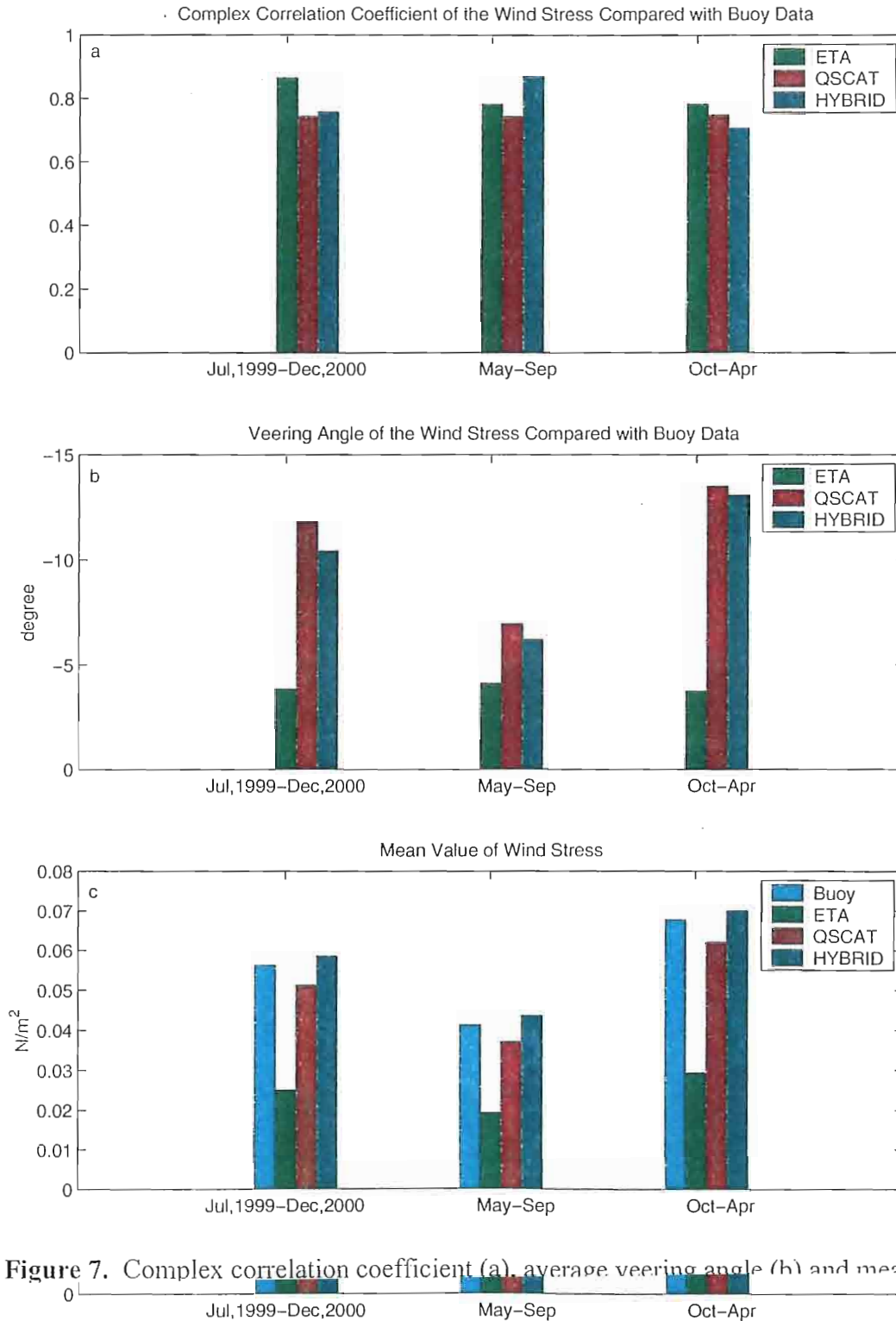


**Figure 7.** Complex correlation coefficient (a), average veering angle (b) and mean value

(c) of wind stress from ETA (green), QSCAT (red) and HYBRID (blue) wind fields compared with buoy observation (cyan) during different time periods at  $28.51^{\circ}$  N,  $84.51^{\circ}$  W.

The Map Where the Four Stations and NDBC Buoy are Located

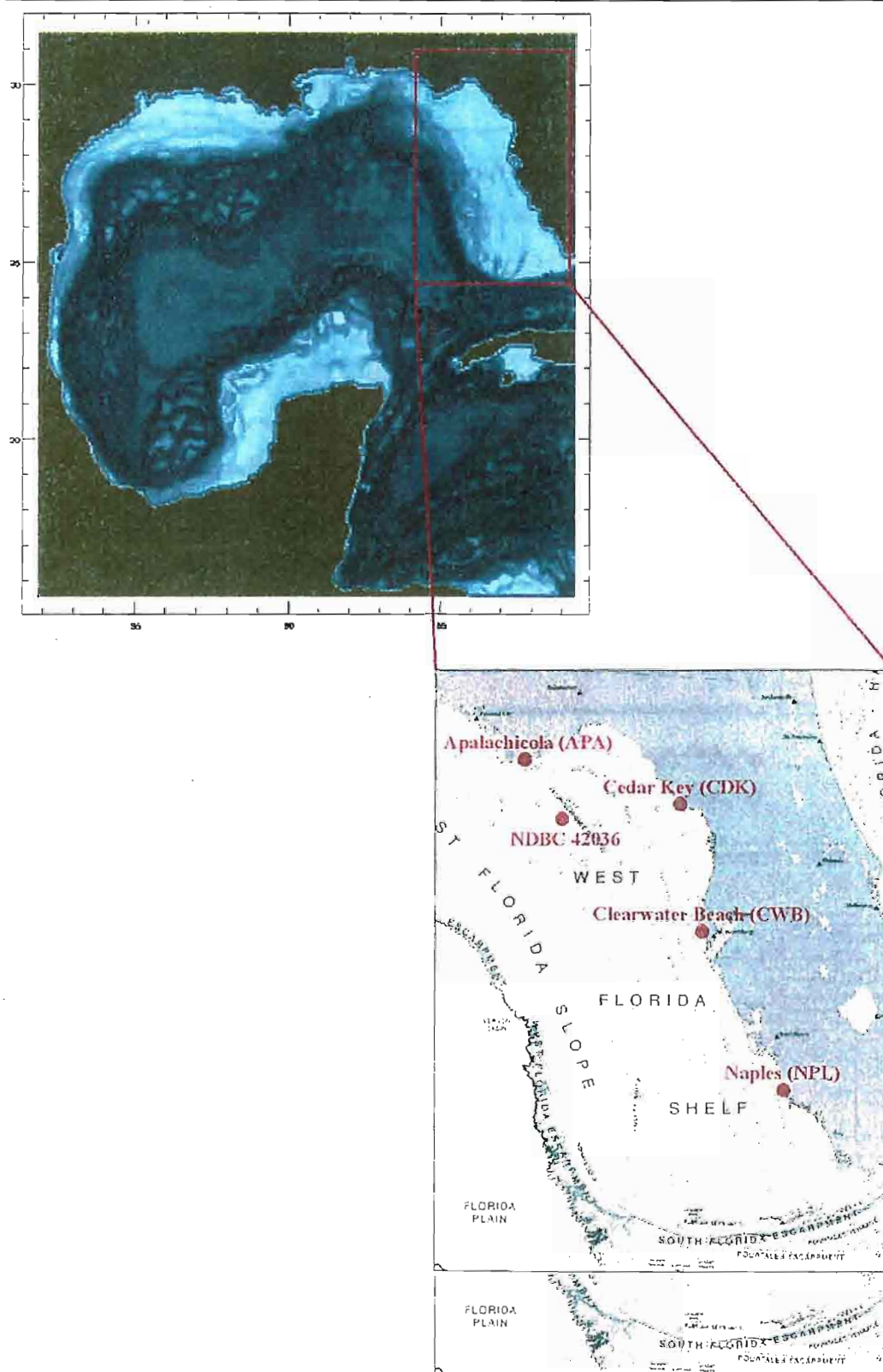


**Figure 8.** Wind data from NDBC 42036 is used to compare with ETA, QSCAT and HYBRID wind fields; SSH data from four stations along the WFS are also examined, they are Apalachicola, Cedar Key, Clearwater Beach and Naples.

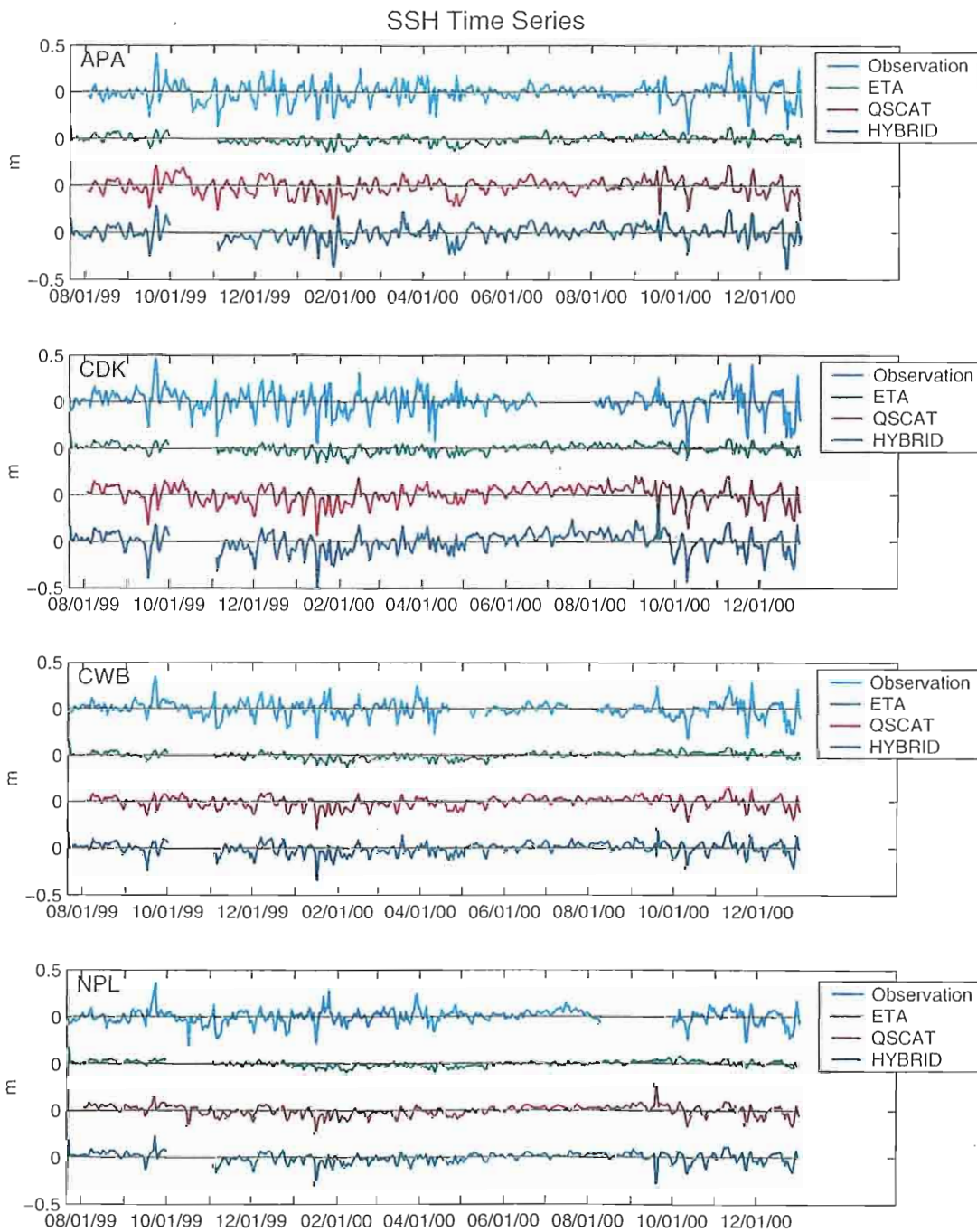


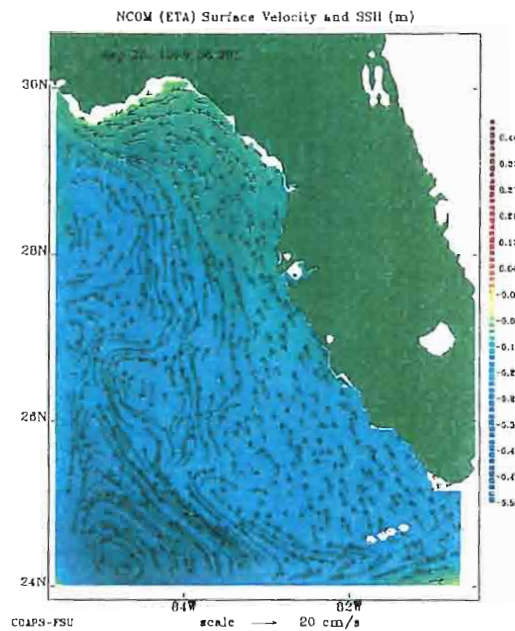
**Figure 9.** Time series of SSH anomaly from observation (cyan), NCOM/ETA (green), NCOM/QSCAT (red) and NCOM/HYBRID (blue) model simulations during July, 1999-

**Figure 9.** Time series of SSH anomaly from observation (cyan), NCOM/ETA (green), NCOM/QSCAT (red) and NCOM/HYBRID (blue) model simulations during July, 1999-Dec, 2000 at four stations: Apalachicola (APA), Cedar Key (CDK), Clearwater Beach (CWB) and Naples (NPL).

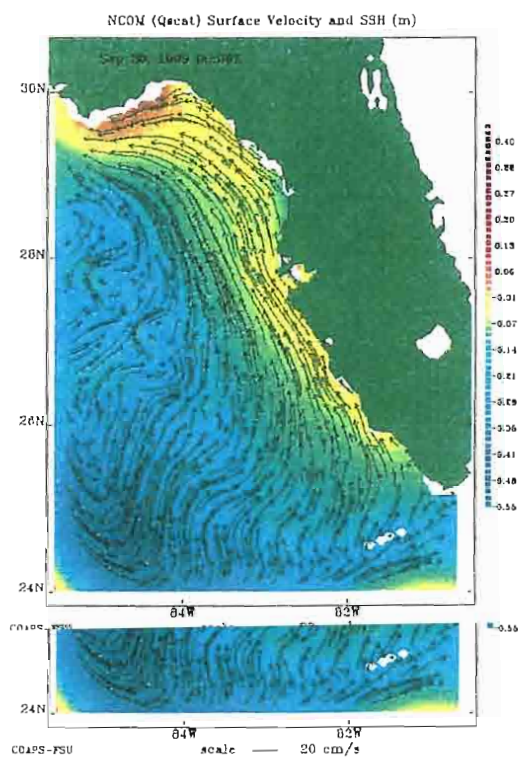
## Snapshots of the SSH Fields

**Figure 10.** Snapshots of the SSH fields on WFS from NCOM/ETA, NCOM/QSCAT and NCOM/HYBRID at 06:00 Z, Sep 20, 1999, which is 6 hour after tropical storm Harvey arrived GoM.

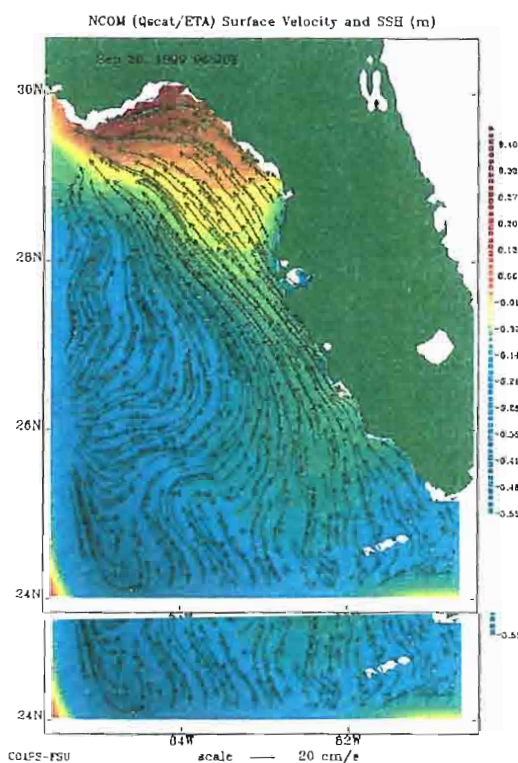
### NCOM/ETA



### NCOM/QSCAT



### NCOM/HYBRID





### SSH Comparison for The Whole Study Time Period

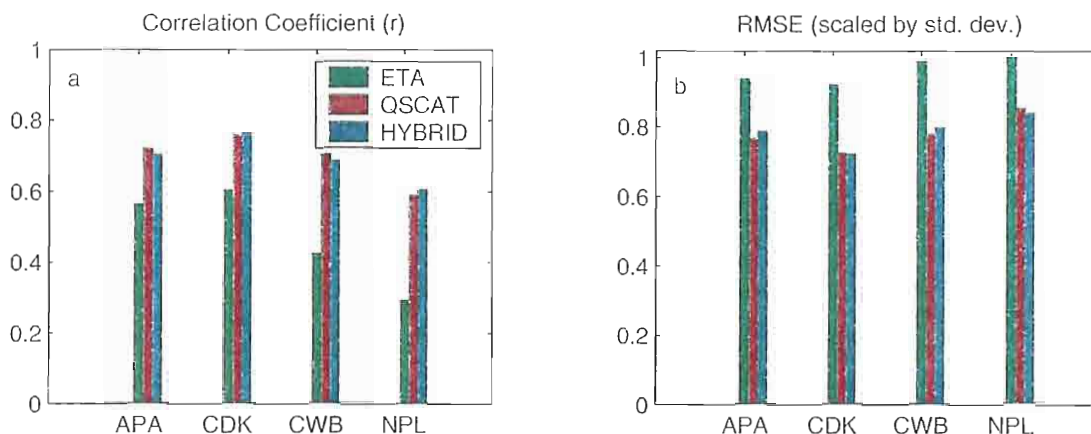


**Figure 11.** Correlation coefficient (a) and RMSE scaled by standard deviation of observed SSH (b) between SSH anomaly from observation and NCOM/ETA (green), NCOM/QSCAT (red) and NCOM/HYBRID (blue) model simulations during July, 1999-Dec, 2000 at four different stations: Apalachicola (APA), Cedar Key (CDK), Clearwater Beach (CWB) and Naples (NPL).

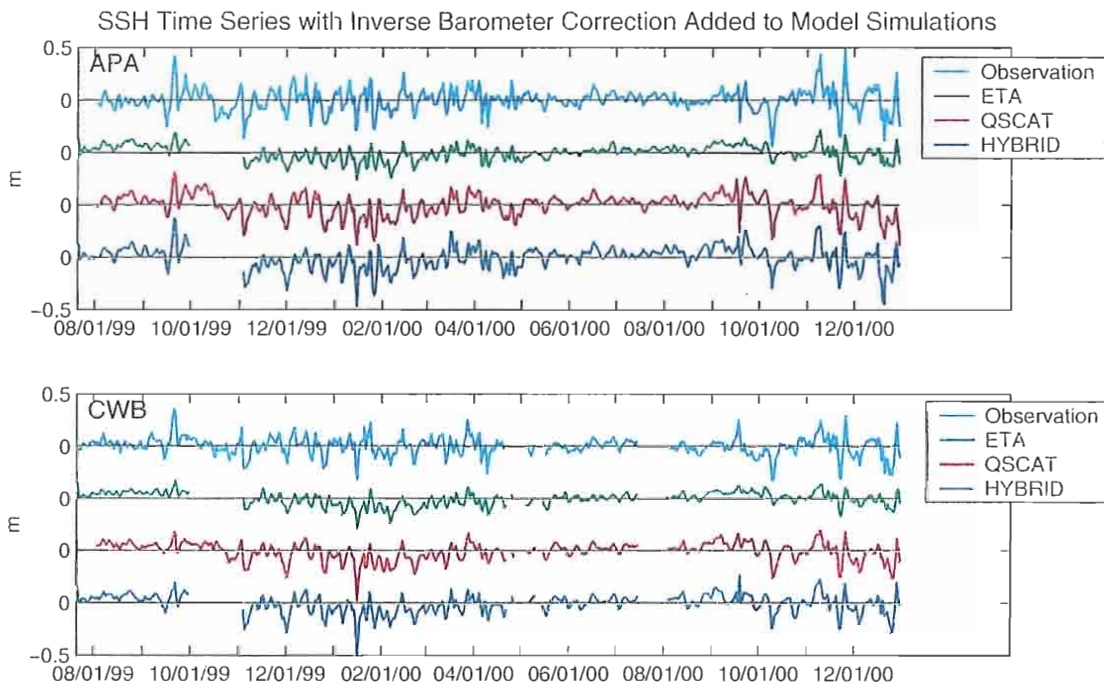


**Figure 12.** Time series of SSH anomaly from observation (cyan), NCOM/ETA (green), NCOM/QSCAT (red) and NCOM/HYBRID (blue) model simulations during July, 1999-Dec, 2000 at four different stations: Apalachicola (APA) and Clearwater Beach (CWB) after inverse barometer correction is added to SSH from model output.

### SSH Comparison for The Whole Study Time Period after Inverse Barometer Correction Being Added

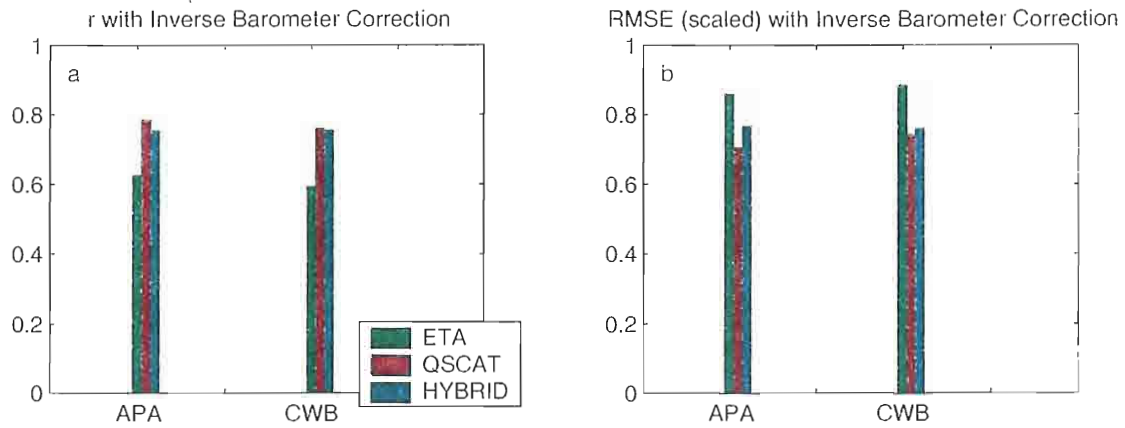


**Figure 13.** Correlation coefficient (a) and RMSE scaled by standard deviation of observed SSH (b) between SSH anomaly from observation and NCOM/ETA (green), NCOM/QSCAT (red) and NCOM/HYBRID (blue) model simulations during July, 1999-Dec, 2000 at four different stations: Apalachicola (APA), Cedar Key (CDK), Clearwater Beach (CWB) and Naples (NPL) after inverse barometer correction is added to SSH from model output.

## SSH Comparison between Different Seasons

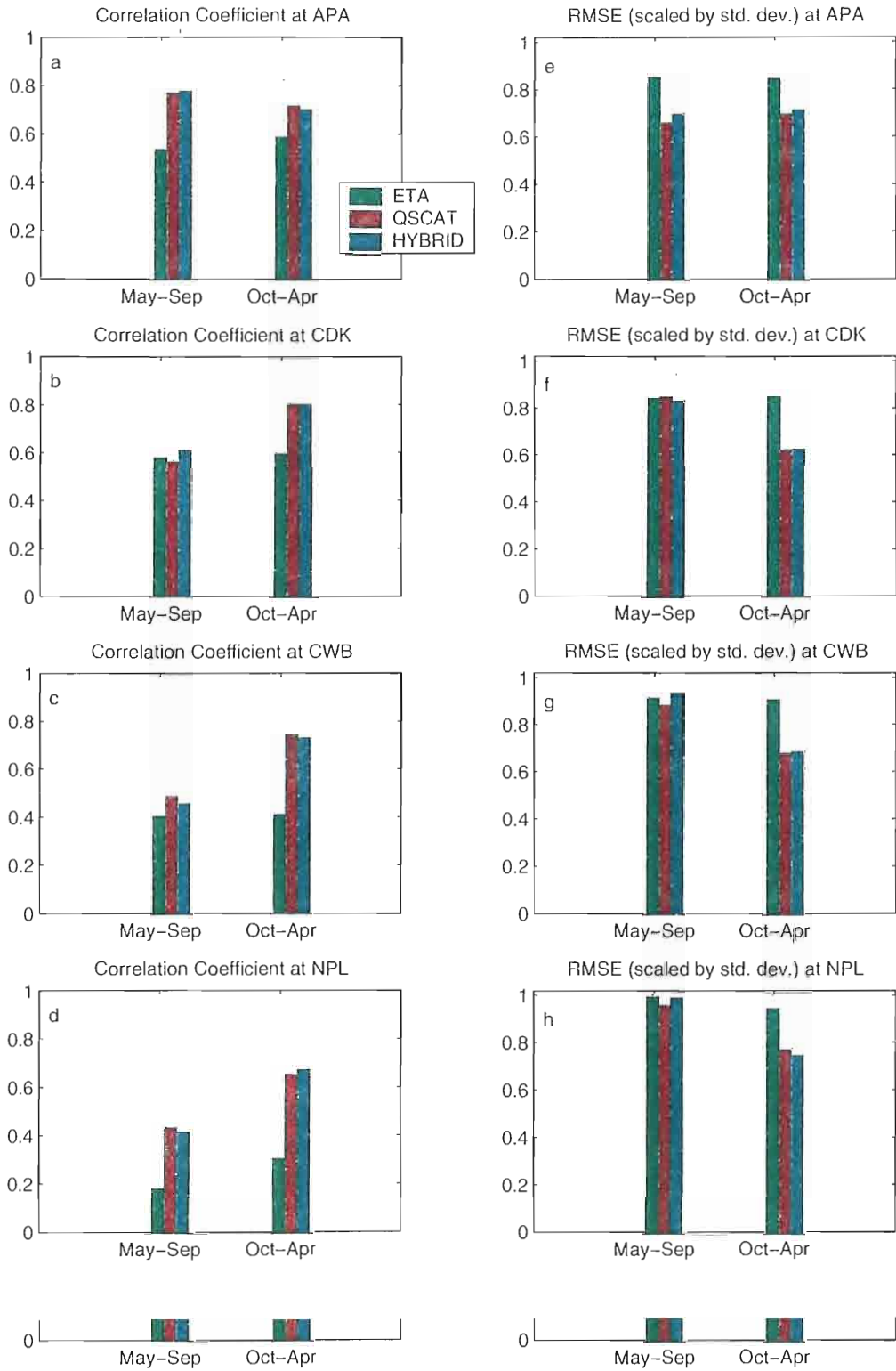


**Figure 14.** Correlation coefficient (a-d) and scaled RMSE (e-h) between SSH anomaly from observation and NCOM/ETA (green), NCOM/QSCAT (red) and NCOM/HYBRID (blue) model simulations during 'May- Sep' and 'Oct- Apr' seasons at four different stations.

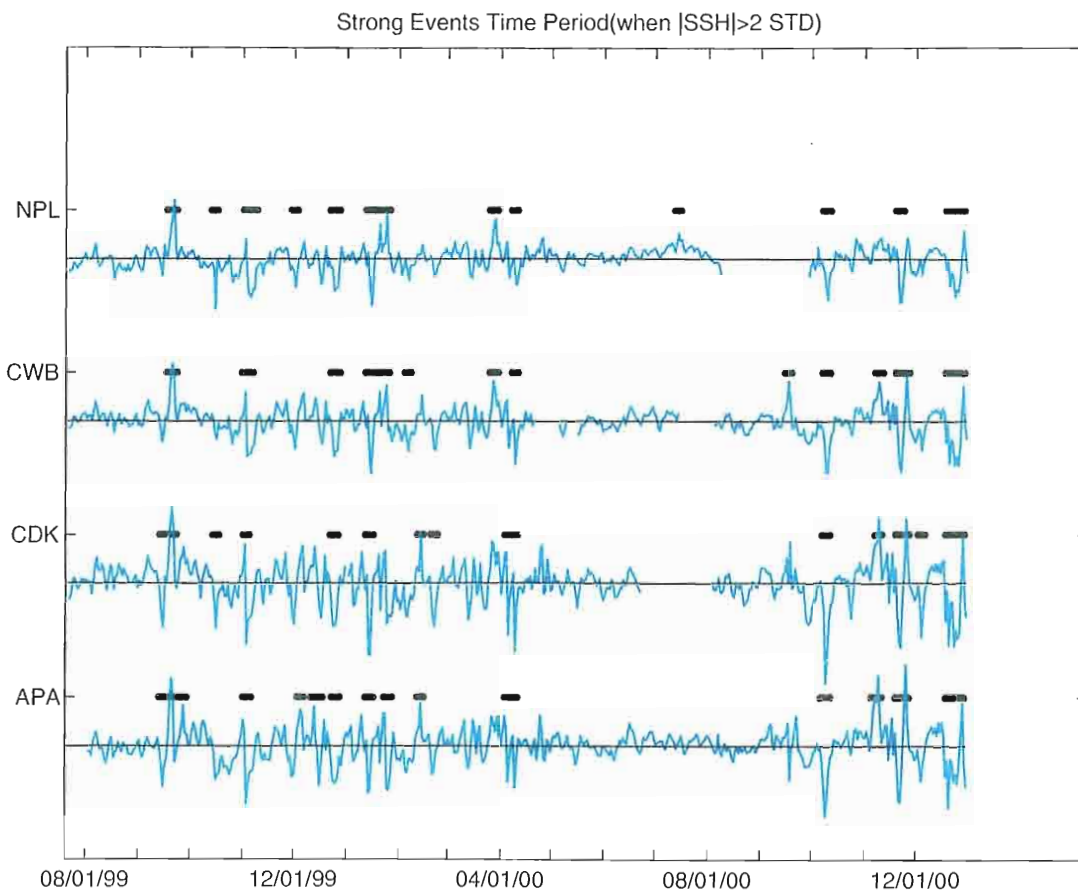


**Figure 15.** Strong event periods when  $SSH \geq 2$  standard deviation of observation (std. dev.) at four stations. When  $SSH \geq 2$  std. dev., a 7 day window is defined. Lines indicate strong event period, which occupies 20% of the whole time period approximately.

## SSH Comparison between “Strong Events” and “Weak Events”

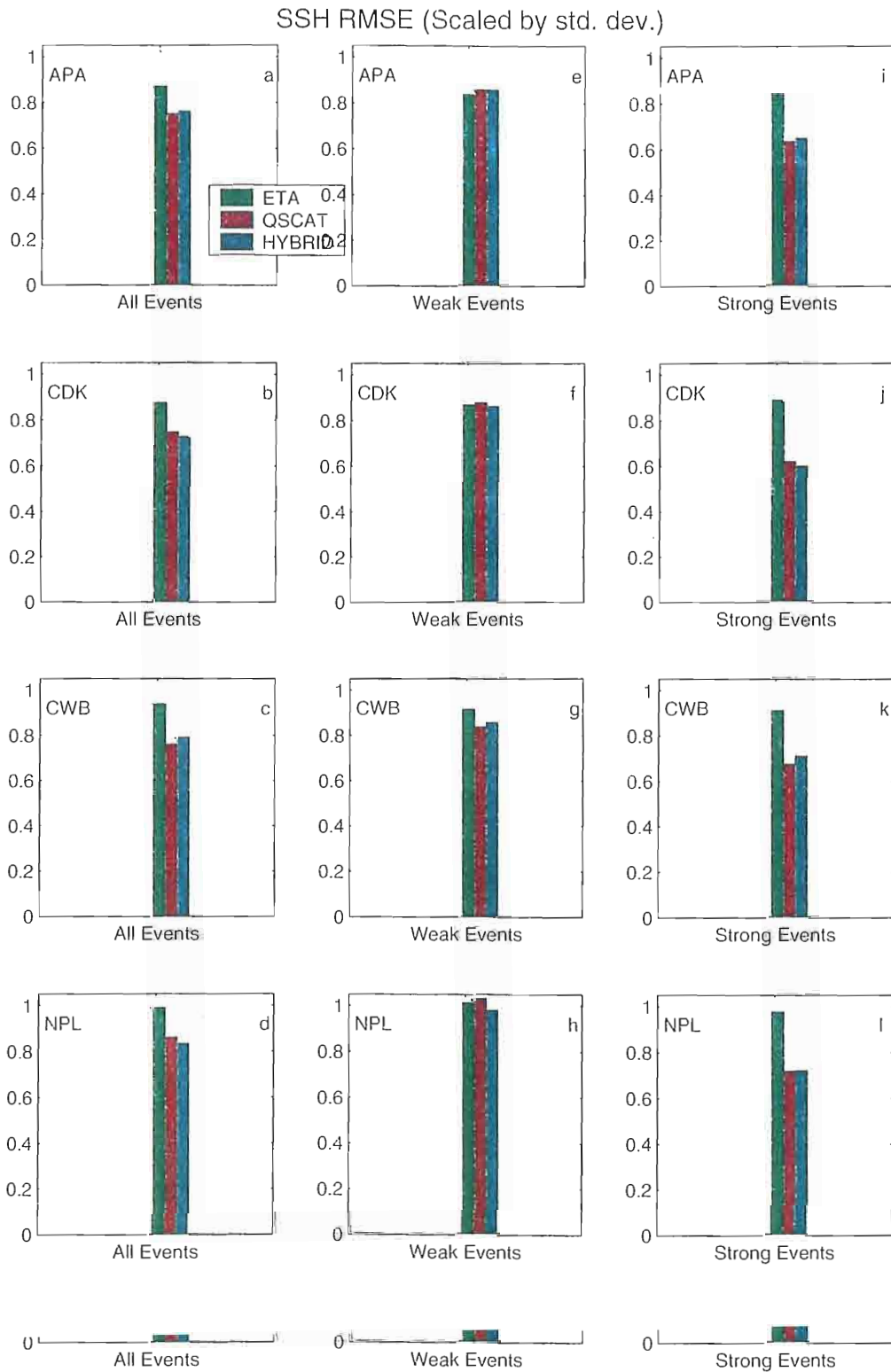


**Figure 16.** Scaled RMSE between SSH anomaly from observation and NCOM/ETA (green), NCOM/QSCAT (red) and NCOM/HYBRID (blue) model simulations calculated for the whole time period (a-d) and during weak events time period (e-h) and strong events time period (i-l) at four different stations.

**Table 1a.** Increase Rate of correlation coefficient of SSH from different model runs with observation after Inverse barometer correction is added to model output during the whole study time period

	<b>NCOM/ETA</b>	<b>NCOM/QSCAT</b>	<b>NCOM/HYBRID</b>
<b>Apalachicola</b>	11%	9%	7%
<b>Clearwater Beach</b>	40%	8%	10%

**Table 1b.** Decrease Rate of RMSEs of SSH from different model runs with observation after Inverse barometer correction is added to model output during the whole study time period

	<b>NCOM/ETA</b>	<b>NCOM/QSCAT</b>	<b>NCOM/HYBRID</b>
<b>Apalachicola</b>	8%	7%	2%
<b>Clearwater</b>	10%	4%	4%
<b>Clearwater Beach</b>	10%	4%	4%

## REFERENCES

- Baumgartner, M. F. and Steven P. Anderson, Evaluation of regional numerical weather prediction model surface fields over the Middle Atlantic Bight, *Journal of geophysical research*, Volume 104, 1999.
- Black , T. L., The new NMC mesoscale Eta model: description and forecast examples, *Weather and forecasting*, Volume 9, 1994.
- Blumberg, A.F. and G.L. Mellor, Diagnostic and prognostic numerical circulation studies of the South Atlantic Bight, *Journal of geophysical research*, Volume 88, 4579- 4592, 1983.
- Blumberg, A.F. and G.L. Mellor, A description of a three-dimensional coastal ocean circulation model. In *Three-Dimensional coastal ocean models*, N. Heaps Ed., American Union, New York, N. Y., 208 pp., 1987.
- Boicourt, W. C., William J. Wiseman, JR., Chapter 6 Continental shelf of the southeastern united states and the gulf of Mexico: In the shadow of the western boundary current, *The sea*, Volume 11, 1998.
- Bourassa, M. A., D. G. Vincent, W. L. Wood, A flux parameterization including the effects of capillary waves and sea state, *Journal of Atmosphere. Science.*, Volume 56, 1123-1139, 1999.
- Chin , T. M., Ralph F. Milliff, and William G. Large, Basin-scale, high-wavenumber sea surface wind fields from a multiresolution analysis of scatterometer data, *Journal of atmospheric and oceanic technology*, Volume 15, 1998.
- Cragg, J., G. Mitchum and W. Sturges, Wind-induced sea surface slopes on the West Florida Shelf, *Journal of physical oceanography*, Volume 13, 1983.
- Grima, N., A. Bentamy, K. Katsaros, Y. Quilfen, Sensitivity of an oceanic general circulation model forced by satellite wind stress fields, *Journal of geophysical research*, Volume 104, C4, 1999.
- Grima, N., A. Bentamy, K. Katsaros, Y. Quilfen, Sensitivity of an oceanic general circulation model forced by satellite wind stress fields, *Journal of geophysical research*, Volume 104, C4, 1999.
- Christopher N. K. Mooers and George A. Maul, Chapter 7. Intra-Americas Sea Circulation, *The sea*, Volume 11, 1998.



- Foreman G.G., Tidal analysis based on high and low water observations, *Pacific marine science report 79-15*, Institute of Ocean Sciences, Patricia Bay, 36 pp, 1996.
- Gilhousen, D.B., A field evaluation of NDBC moored buoy winds, *J. Atmos. Oceanic Technol.*, Volume 4, 94-104, 1987.
- Hackert, E.C., A.J. Busalacchi, and R. Murtugudde, A wind comparison study using an ocean general circulation model for the 1997-98 El Niño. *J. Geophys. Res.*, Volume 106, 2345-2362, 2001.
- Holland, W. R., J. C. Chow, and F.O. Bryan, Application of a third-order upwind scheme in the NCAR ocean model, *Journal of climate*, 11, 1487-1493, 1998.
- Kundu, P. K. Ekman veering observed near the ocean bottom, *Journal of physical oceanography*, volume 6, 1976.
- Large, W.G. and G.B. Crawford, Observations and simulations of upper ocean response to wind events during the Ocean Storms experiment, *Journal of physical Oceanography*, Volume 25, 1995.
- MarMorino. G. O., Variability of current, temperature, and bottom pressure across the West Florida continental shelf, winter 1981-1982 and 1983, Cragg et al. 1983, *Journal of geophysical research*, Volume 88, 1983.
- Martin, P.J., Testing and comparison of several mixed-layer models, NORDA report 143, *Naval research laboratory, Stennis space center, Miss.*, 1998.
- Martin, P. J., Description of the Navy Coastal Ocean Model Version 1.0, *Navy Research Laboratory, Stennis space center, Miss.*, 30 pp., 2000.
- Nicholls, R. J., Improved estimates of coastal population and exposure to hazards released, *EOS, Transactions, American geophysical union*, Volume, 83, 9 July 2002.
- Milliff, R. F., William G. Large, Jan Morzel, and Gokhan Danabasoglu, Ocean general circulation model sensitivity to forcing from scatterometer winds, *Journal of geophysical research*, Volume, 104, 11337-11358, 1999.
- Pegion, P.J., M. A. Bourassa, D. M. Legler, and J. J. O'Brien, Objectively derived daily "winds" from satellite scatterometer data, *Monthly weather review*, Volume 128, 2000.
- Spencer, M.W., NASA Scatterometer near-real-time, value added products for meso/synoptic-scale marine forecasting, *IGARSS '96, 1996 International Geoscience and Remote Sensing Symposium, Remote Sensing for a Sustainable Future* (Cat. No.96CH35875), p. 4 vol. lxxi+2383, 82-4 vol.1, 1996.

Verschell, M. A., M. A. Bourassa, D. E. Weissman, and J. J. O'Brien, Model validation of the NASA scatterometer winds, *Journal of geophysical research*, Volume 104, 11,359-11,374, 1999.

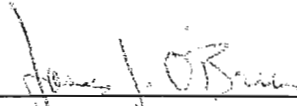
Weisberg, R. H., Zhenjiang Li, and Frank Muller-Karger, West Florida shelf response to local wind forcing: April 1998, *Journal of geophysical research*, Volume 106, 2001.

## BIOGRAPHICAL SKETCH

Xujing Jia, the daughter of Yuzhi Liu and Chunsheng Jia, was born in the town of Zhenxiang, on the plains of the Heilongjiang Province of Northeastern China on June 18, 1974. Upon finishing high school, she moved to the coastal city of Qingdao to study at the renowned Ocean University of Qingdao. She earned both a Bachelor's degree and a Master's degree in Marine Meteorology from Ocean University in 1997 and 2000 respectively. Her Master's thesis research has been published in several journals before coming to the USA as a graduate student in Physical Oceanography at Florida State University.

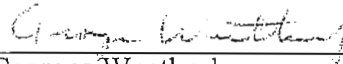
During her stay at FSU, Xujing was engaged in activities associated with the Physical Oceanography Department, and the Chinese Student Association amongst other things. She also met her amazing husband, Shannon, during this time. In the Fall, 2002 term, they will begin a new chapter together as Ph.D. students in Physical Oceanography elsewhere.

The members of the Committee approve the thesis of Xujing Jia  
defended on July 19, 2002



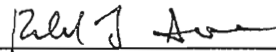
---

James J. O'Brien  
Professor Directing Thesis



---

Georges Weatherly  
Committee Member



---

Richard Iverson  
Committee Member

Approved:



---

David Thistle, Chair, Department of Oceanography



---

David Thistle, Chair, Department of Oceanography